https://doi.org/10.5194/essd-2024-291
Preprint. Discussion started: 9 August 2024


Earth System Science Data
Open Access Discussions

# Gap-Filling for Daily Evapotranspiration Observations with full-factorial method at Global Flux Sites

Xiaowei Wang[1, 2], Fujiao Tang[3], Yazhen Jiang[1, 4*], Yunsheng Lou[2]

[1]State Key Laboratory of Resources and Environment Information System, Institute of Geographic Sciences and Natural Resources Research, Chinese Academy of Sciences, Beijing 100101, China;
[2]School of Ecology and Applied Meteorology, Nanjing University of Information Science & Technology, Nanjing 210044, China;
[3]School of Transportation Science and Engineering, Harbin Institute of Technology, 150090 Harbin, China;
[4]University of Chinese Academy of Sciences, Beijing 100049, China.

*Correspondence to*: Yazhen Jiang (jiangyz@lreis.ac.cn)

**Abstract.** Evapotranspiration (ET) plays a crucial role in the regional water-energy cycle, illustrating intricate interactions among climate, vegetation and soil. Eddy covariance (EC) technology is a primary method for measuring ET. However, data gaps commonly result from adverse weather conditions and equipment malfunctions. This study utilizes the full-factorial method to address the ET gaps at 339 sites across multiple global flux networks. The filled ET data are then compared with three ET products: the Land component of the Fifth Generation of European Reanalysis (EAR5-Land), the Global Land Evaporation Amsterdam Model (GLEAM), and the Breathing Earth System Simulator (BESS). The results indicate a high level of consistency between the filled ET data and the three ET products at 264 out of the 339 sites. The absolute average mean error (|MAE|) is 0.32 mm/d, and the root mean square error (|RMSE|) is 0.92 mm/d. Among the remaining 75 sites, 49 exhibit better agreement between filled ET and measured ET data than ET products, both in terms of seasonal variations and numerical ranges. Further verification is required for the reliability of filled ET data at the remaining 26 sites, due to the limited availability of measured ET data. Overall, the gap-filled ET data from 313 sites (2210 site-years) demonstrate high-quality. These sites exhibit a strong correlation between available energy and turbulent fluxes, with $R^2$, MAE, and RMSE for different surface types ranging from 0.84 to 0.94, 21.49 to 28.67 W/m², and 28.37 to 36.91 W/m², respectively. The average energy balance closure rate is 0.73, indicating a relatively high degree of closure in the energy balance. These 313 sites, featuring high-quality filled ET data, can be utilized for ET model validation, ET product verification, water demand assessment, and other related tasks. The filled ET dataset can be publicly accessed at https://doi.org/10.57760/sciencedb.11651 (Wang & Jiang, 2024).

https://doi.org/10.5194/essd-2024-291
Preprint. Discussion started: 9 August 2024


## 1 Introduction

Evapotranspiration (ET) describes the phase transition of water from liquid to gas at the surface, and plays a central role in linking the water, energy and carbon cycles (Amani & Shafizadeh-Moghadam, 2023; Zhang et al., 2024). As the second-largest terrestrial hydrological flux following precipitation, ET returns over 60% of incident precipitation to the atmosphere and contributes approximately 50% of net surface radiation as latent heat flux (Mu et al., 2011; Rummler et al., 2019). Tightly integrated with the carbon cycle, ET regulates weather forecasting, agricultural irrigation, and ecosystem health through the simultaneous control of plant stomatal activities on transpiration and photosynthesis (Aouissi et al., 2016; Graveline et al., 2024; Li et al., 2021). Therefore, long-term and effective observations of ET are crucial for advancing our understanding of dynamics in water budget, energy balance, and carbon cycle (Valentín et al., 2023; Zheng et al., 2023).

Although a plethora of ET products has been developed, each is grounded in distinct algorithms that include empirical formulas (Bhattarai et al., 2019; Wan et al., 2015), physical models (Long et al., 2014; Wang & Dickinson, 2012), or machine learning-based methods (Amani & Shafizadeh-Moghadam, 2023; Granata, 2019). These products address various parameterized issues such as vegetation cover, soil moisture, and atmospheric conditions (Drexler et al., 2004; Koppa et al., 2022; Başakın et al., 2023; Allen et al., 2011). Regional and global assessments have unveiled significant disparities among these ET products (Xiong et al., 2021; Wu et al., 2023; Kim et al., 2021; Qian et al., 2023), highlighting the absence of a universally accepted standard for precise in ET estimation (Zhang et al., 2016; Li et al., 2018; Xie et al., 2024; Tang et al., 2024; Zhu et al., 2022b; Polhamus et al., 2013; Nkiaka et al., 2022). Consequently, the integration and utilization of reliable measured ET data for comparative validation becomes a pivotal step toward enhancing the accuracy and credibility of ET data for applications related to water cycle and energy balance.

The eddy covariance (EC) method, which quantifies latent heat flux, the energy expression of ET, by determining the covariance among vertical wind speed, temperature, and water vapor mixing ratio over a designated averaging period, is considered one of the most direct and dependable techniques for flux measurement (Chen et al., 2012). Major global EC flux networks including FLUXNET, AmeriFlux, OzFlux, EuroFlux, AsiaFlux, and ChinaFlux systematically gather latent heat flux across more than 1,000 sites characterized by diverse land cover types (Helbig et al., 2021). Nevertheless, the continuity of these observations is frequently interrupted by several factors including instrument malfunctions, severe meteorological conditions, and maintenance disruptions. As a result, the complete coverage of ET data obtained from most flux network sites typically ranges between 65% to 75%, and this issue has been extensively documented (Falge et al., 2001b; Majozi et al., 2017). For instance , at an EC site located on the southeastern United States coastal plain, the average nighttime data gap rate is 60% (Kunwor et al., 2017). At the Walker Branch Watershed AmeriFlux site, approximately 22% of the half-hour daytime ET measurements exhibit data gaps (Wilson & Baldocchi, 2001), while this figure rises to 35% at

https://doi.org/10.5194/essd-2024-291
Preprint. Discussion started: 9 August 2024


the Duke site (Katul et al., 2001), and remains 20% at the Niwot Ridge site (Monson et al., 2002). These data gaps hinder detection of shifts in ET, precipitation, and land water availability (Morton, 1983), significantly affecting the accuracy of water resource management and hydrological models (Talib et al., 2024; Wu et al., 2021), also pose challenges for scientists in precisely assessing the impacts of climate change on the water and carbon cycles (Govender et al., 2022; Novick et al., 2022).

Several methods have been developed to fill gaps in EC measured ET, enabling the acquisition of extended and continuous observational datasets. These methods mainly include the look-up table (Falge et al., 2001b), the statistical filter (Jarvis et al., 2004), the marginal distribution sampling (Wutzler et al., 2018), the multivariate analysis (Stauch & Jarvis, 2006), the mean diurnal variation (MDV) (Falge et al., 2001a), the marginal distribution sampling (MDS)(Foltýnová et al., 2020; Yeonuk et al., 2020), and the process-based model (Xing et al., 2008). Although exiting methods offer viable solutions for filling ET gaps, most lack a robust physical foundation and largely rely on the selection of specific inputs or possess complex model structures. Furthermore, the required input data for these methods are often difficult to obtain, which compromises their applicability and reduces their spatiotemporal scalability. For instance, Pastorello et al. (2020) employed the MDS method to fill gaps in the FLUXNET dataset's ET observations, based on the assumption that ET remains consistent under similar meteorological conditions over short intervals (El-Madany et al., 2018). Nonetheless, the validity of this method may be compromised by sudden shifts in soil moisture, even under stable meteorological conditions (Alavi et al., 2006). Moreover, the MDS method faces significant uncertainties when addressing long ET gaps (Zhu et al., 2022a), which undermines the overall reliability of the FLUXNET dataset. Given the constraints and drawbacks of these methods, there exists a notable deficiency in the availability of comprehensive gap-filled ET datasets; to our knowledge, only one such dataset, published by Winck et al. (2023), has been identified. Recently, Jiang et al. (2022) proposed a full-factorial method based on the physical mechanism of the Penman-Monteith equation, incorporating a full range of influential factors of the overall ET. The full-factorial method has demonstrated superior logicality and reasonableness in its underlying mechanisms, surpassing various other gap-filling methods that do not fully incorporate influential ET factors. Additionally, this approach shows enhanced accuracy in filling gaps on both hourly and daily scales, with a bias range between 1.9 $W/m^2$ and 2.9 $W/m^2$, and a root mean square error range between 18.8 $W/m^2$ and 25.0 $W/m^2$ (Jiang et al., 2022).

Aiming to compile a comprehensive gap-filled ET dataset, we address the ET data gaps using the full-factorial method across global flux networks, thereby facilitating the acquisition of high-frequency EC time series data for ET. This study encompasses the following primary objectives: (1) processing of site data from multiple source flux networks; (2) gap-filling of ET at each site with the full-factorial method; and (3) verification and comparative analysis of the filled ET data against three ET products.

https://doi.org/10.5194/essd-2024-291
Preprint. Discussion started: 9 August 2024


## 2 Methodology and data

### 2.1 Full-factorial method and Gap-Filling schedule

#### 2.1.1 Full-factorial method

The Full-factorial gap-filling method, which was physically based, was implemented using the decoupled model from the Penman-Monteith equation (Jiang et al., 2022). This method synthesizes various factors, including atmospheric, vegetation, and soil conditions, to proficiently simulate the intricate mechanisms impacting ET. The gap-filled ET with this scheme is described as follows:

$$ET_{\mathrm{gap}} = ET_{\mathrm{obs}} \frac{(R_n - G)_{\mathrm{gap}}}{(R_n - G)_{\mathrm{obs}}} \frac{\Delta_{\mathrm{gap}}}{\Delta_{\mathrm{obs}}} \frac{(\Delta+\gamma)_{\mathrm{obs}}}{(\Delta+\gamma)_{\mathrm{gap}}} \frac{\beta^*_{obs}}{\beta^*_{\mathrm{gap}}} \quad (1)$$

$$\beta^* = \left[1 + \frac{\rho C_p VPD}{(R_n - G) r_a}\right]^{-1} \quad (2)$$

$$\Delta = \frac{4098 \times e_s(Ta)}{(Ta + 237.3)^2} \quad (3)$$

$$e_s(Ta) = 0.6108 \times \exp\left(\frac{17.27 \times Ta}{T + 237.3}\right) \quad (4)$$

$$p = \frac{P}{R \cdot (T + 273.15)} \quad (5)$$

$$\gamma = \frac{C_p \times P}{\varepsilon \times \lambda} \quad (6)$$

$$ra = \frac{\ln\left(\frac{Z-d}{z_{0m}}\right) \times \ln\left(\frac{Z-d}{z_{0h}}\right)}{k^2 \times u} \quad (7)$$

$$d = 6.67 * z_{0m} \quad (8)$$

$$\mathrm{z}_{oh} = 0.1 * z_{0m} \quad (9)$$

https://doi.org/10.5194/essd-2024-291
Preprint. Discussion started: 9 August 2024


Open Access Earth System Science Data Discussions

where the subscript 'obs' refers to observed values, and 'gap' indicates the missing data; β* represents the decoupling coefficient when ET equals the equilibrium evaporation; $\Delta$ (kPa/K) is the slope of the air temperature–saturation vapor pressure relation; $\gamma$ (kPa/K) is the psychrometric coefficient; $R_n$ (W/m$^2$) is the net radiation; $G$ (W/m$^2$) is the soil heat flux; $VPD$ (kPa) is the vapor pressure deficit of air; $ra$ (s/m) is the aerodynamic resistance; $Ta$ (°C) is the air temperature; $e_s$ (kPa) is the saturated water vapor pressure; $p$ (kg/m$^3$) is the air density; $P$ (kPa) is the atmospheric pressure; $R$ (kJ/kg·K) is the ideal gas constant, valued at 0.287; $C_p$ (kJ/kg·K) is the specific heat capacity of air, valued at 1.004; $\varepsilon$ is the ratio of the specific heat capacities of moist air to dry air, valued at 0.622; $\lambda$ (kJ/kg) is the latent heat of vaporization of water, valued at 2.45; $k$ is the von Kármán constant, valued at 0.41; $u$ (m/s) is the wind speed; $Z$ (m) is the measurement height of wind speed (10 m in this study); $d$ (m) is the zero-plane displacement height; $z_{0m}$ (m) is the roughness length for momentum transfer; and $z_{0h}$ (m) is the roughness length for heat transfer.

#### 2.1.2 Gap-Filling schedule

In this study, data on ET and associated meteorological variables from global flux sites are initially reprocessed, including resampling and quality control, to simultaneously identify the data gaps. Subsequently, reanalysis products are utilized to fill gaps in the meteorological data from these networks. This step is crucial, as the full-factorial method, which relies on meteorological variables as input, cannot address ET data gaps when related variables are also incomplete. To evaluate whether the full-factorial method retains its efficacy in filling ET gaps within datasets that have been filled with meteorological reanalysis products, specific gaps were randomly created and tested within the measured ET values. Finally, the full-factorial method was applied to fill these gaps across various sites, and the filled data were compared with three ET products using diverse evaluation metrics. Sites exhibiting high consistency between the filled data and ET products were deemed to have high quality filled ET data. For sites with notable discrepancies, the causes were investigated by analysing the seasonal changes in measured ET, net radiation (Rn), and leaf area index (LAI), alongside the numerical range of measured ET on a site-specific scale. This analysis aids in further identifying which sites possess high-quality filled ET data. Additionally, the energy closure ratio and the spatial and temporal distribution of the filled data were analysed to deepen understanding of their characteristics. Figure 1 illustrates the gap-filling schedule flowchart for this study.

https://doi.org/10.5194/essd-2024-291
Preprint. Discussion started: 9 August 2024


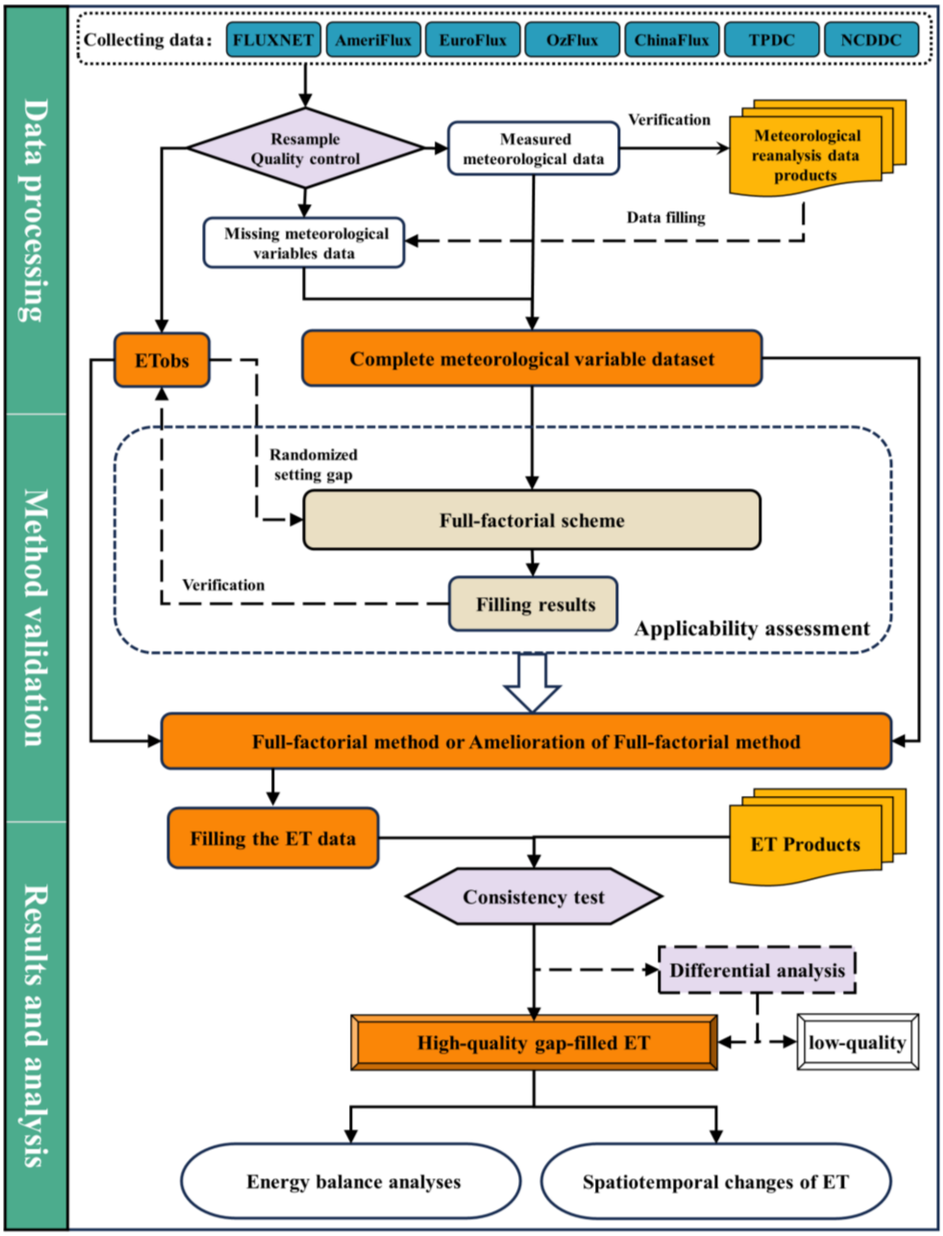


**Figure 1: Flowchart of the Gap-Filling schedule.**

https://doi.org/10.5194/essd-2024-291
Preprint. Discussion started: 9 August 2024


## 2.2 Data

### 2.2.1 Evapotranspiration observations

ET observations are collected from global flux networks including: AmeriFlux (https://ameriflux.lbl.gov, since 1991, with 444 sites recording data over periods ranging from 1 to 32 years) (Novick et al., 2018); FLUXNET (https://fluxnet.org, since 1991, featuring over 1000 active and historical sites with data time series lengths from 1 to 22 years) (Pastorello et al., 2020); EuroFlux (http://www.europe-fluxdata.eu, since 1996, with 487 sites); OzFlux (https://ozflux.org.au, since 2001, with 34 sites during from 3 to 22 years) (Beringer et al., 2016); ChinaFlux (http://www.chinaflux.org), National Tibet Plateau Data Center (TPDC, https://data.tpdc.ac.cn), and the National Cryosphere Desert Data Center (NCDDC, http://www.ncdc.ac.cn, since 2002, totalling 79 sites with data recording periods from 1 to 23 years) (Pan et al., 2021; Yu et al., 2006a, b). These networks and data centres constitute a global database that provides high-quality and long-term observational data. From this resource, we collected half-hourly or daily ET measurements and meteorological data from 212 sites within FLUXNET, 195 sites within AmeriFlux, 172 sites within EuroFlux, 22 sites within OzFlux, and 44 sites across ChinaFlux, TPDC, and NCDDC. All these details are provided in Supplementary Table 1 (S1).

### 2.2.2 Meteorological reanalysis data

Meteorological Reanalysis data, including the Land component of the Fifth Generation of European Reanalysis (ERA5-Land), the Global Land Data Assimilation System (GLDAS), and the Modern-Era Retrospective analysis for Research and Applications Version 2 (MERRA-2) are utilized for gap filling in meteorological data at various sites.

Meteorological reanalysis data from ERA5-Land, which offers global coverage at an approximately 9-kilometer resolution with hourly updates, is employed in this study to address missing data in temperature, relative humidity, vapor pressure deficit, atmospheric pressure, net radiation, and wind speed. Ground heat flux data from the GLDAS are utilized to address the gaps in ground heat flux data at EC observation sites. The Catchment Land Surface Model (CLSM), a principal surface models employed by GLDAS, operates with a daily temporal resolution and a spatial resolution of 0.25°. The GLDAS CLSM V2.0 spans from January 1, 1994, to January 31, 2003, while V2.2 extends from February 1, 2003, to December 31, 2023, ensuring continuous data coverage from 1994 through 2023. Data from MERRA-2, an advanced global atmospheric reanalysis project initiated by the National Aeronautics and Space Administration (NASA), includes the M2T1NXFLX dataset, specifically designed for surface flux data with a spatial resolution of 0.5° × 0.625°. This data is used to calculate aerodynamic resistance using $Z_{0m}$ data.

https://doi.org/10.5194/essd-2024-291
Preprint. Discussion started: 9 August 2024


#### 2.2.3 Evapotranspiration products

ET products from the Breathing Earth System Simulator Version 2.0 (BESSv2.0), the Global Land Evaporation Amsterdam Model (GLEAM), and the ERA5-land are utilized for intercomparison with gap-filled ET. Specially, BESSv2.0 provides ET product with a fine spatial resolution of 0.05° and daily temporal resolution, covering the period from 1982 to 2019. GLEAM v3 consistently maintains high standards in ET flux data accuracy, achieving an average correlation coefficient ranging between 0.78 and 0.81 against EC measurements. With a spatial resolution of 0.25°, it spans from 1980 to 2022 and provides ET on daily, monthly, and annual time scales. ERA5-Land delivers ET products at a spatial resolution of 9 kilometres and an hourly temporal resolution.

## 3 Data preprocessing and gap-filling evaluation

### 3.1 Data preprocessing

#### 3.1.1 Evapotranspiration observations processing

In this study, the processing of ET observations involves data resampling, data fusion, and quality control. ET data from the EuroFlux, OzFlux, ChinaFLUX, TPDC and NCDDC sites are initially provided on a half-hourly scale. The same averaging resampling method is applied to resample these data to a daily scale, contingent upon the availability of all 48 half-hourly records within a day. As some sites appear repeatedly across multiple flux networks with varying data length, data fusion is performed to consolidate these sites. Ultimately, we compiled data from 339 sites with daily measured ET and associated meteorological variables. Table S1 in the Supplementary Information details the geographic coordinates, land-cover types (MODIS IGBP) and temporal coverage of these 339 sites. These sites are categorized into various vegetation types as follows: 138 forest sites (DBF/DNF/EBF/ENF/MF); 33 shrubland sites (CSH/OSH); 87 grass sites (GRA/SAV/WSA); 46 crop sites (CRO/CVM); 29 wetland sites (WET); and 6 sites of other types (BAR/SNO/URB/WAT). Figure 2 illustrates the geographic distribution of these sites.

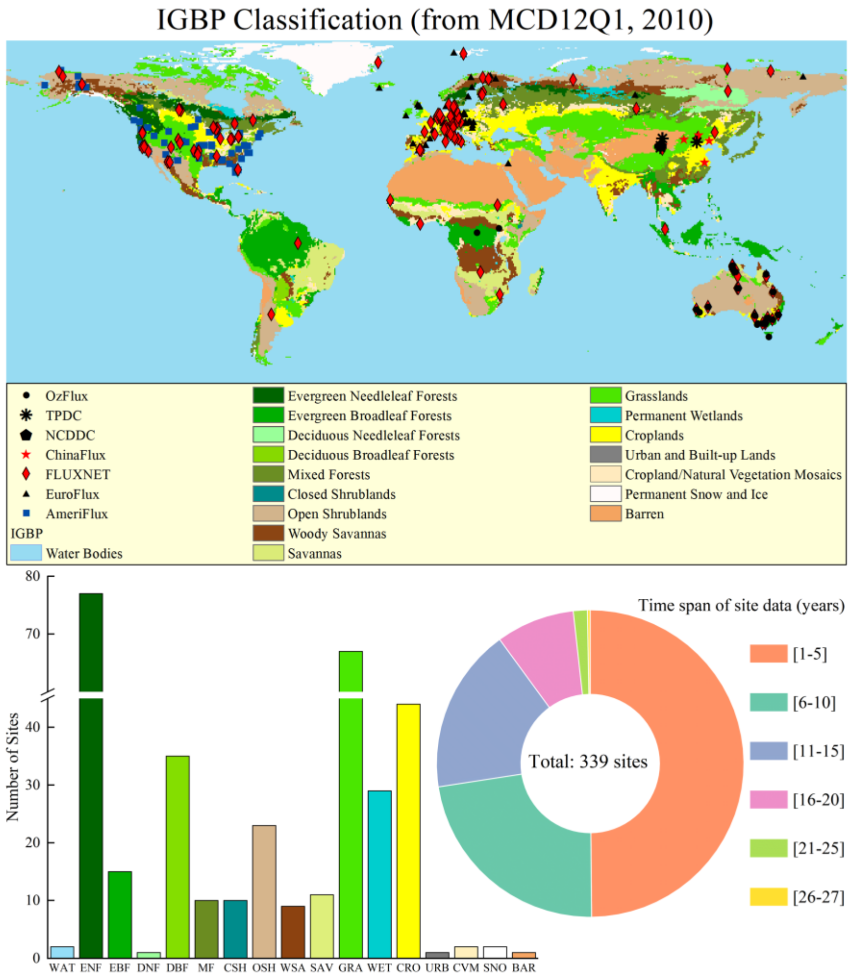


**Figure 2: Distribution of global flux sites by IGBP classification and their data time span.**

We performed quality control on observation data from 339 sites, ensuring that variable values fell within reasonable numerical ranges (as detailed in Table 1), and then assessed the extent of data missingness for each variable (as depicted in Figure 3). The figure reveals that the average gap percentage for air temperature (TA) is the lowest, at approximately 20%, while for vapor pressure deficit (VPD), it is the highest, exceeding 60%. Relative humidity (RH), atmospheric pressure (PA), and wind speed (WS) have similar average gap percentages of around 30%. The average gap percentage for ground heat flux (G) is approximately 40%, and for net radiation (Rn), it exceeds 50%. Similarly, the proportion of gaps in the ET observations is also very high, reaching 50%. These findings underscore the importance of addressing gaps in ET and other variables in EC measurements.

https://doi.org/10.5194/essd-2024-291
Preprint. Discussion started: 9 August 2024


Table 1: Standards for data quality control

| Variables | Min value | Max value | Unit |
|---|---|---|---|
| TA | -50 | 50 | ℃ |
| PA | 70 | 110 | kPa |
| WS | 0 | 20 | m/s |
| RH | 0 | 100 | % |
| VPD | 0 | 5 | kPa |
| Rn | -100 | 700 | $W \cdot m^{-2}$ |
| G | -100 | 200 | $W \cdot m^{-2}$ |
| ET | -100 | 700 | $W \cdot m^{-2}$ |

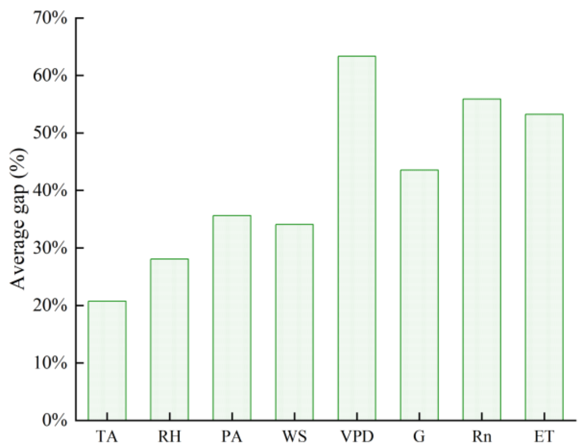


**Figure 3: Average percentage of data gaps for ET and other meteorological variables.**

### 3.1.2 Gap-filling of Meteorological data

Table S2 outlines the methods for calculating meteorological variables from reanalysis product data. To verify the accuracy of the reanalysis products, we randomly sampled 10% of the site's measurement data for comparison, as depicted in Figure 4. The result indicate a high degree of consistency between the measured data for TA, RH, VPD, PA, and Rn and the calculations based on reanalysis products, with an average coefficient of determination ($R^2$) of 0.92. The $R^2$ values for WS, and G are relatively lower, at 0.6 and 0.53 respectively. Nonetheless, the overall accuracy remains relatively high, with the mean absolute error (MAE) and root mean square error (RMSE) between WS and the measurements being 1.02 $m \cdot s^{-1}$ and 1.37 $m \cdot s^{-1}$, respectively, and between G and the measurements being 7.84 $W/m^2$ and 11.93 $W/m^2$, respectively. This indicates good accuracy, confirming that and the three reanalysis products were effectively used to fill the gaps in the meteorological observations at the site scale.

https://doi.org/10.5194/essd-2024-291
Preprint. Discussion started: 9 August 2024

Open Access Earth System Science Data Discussions

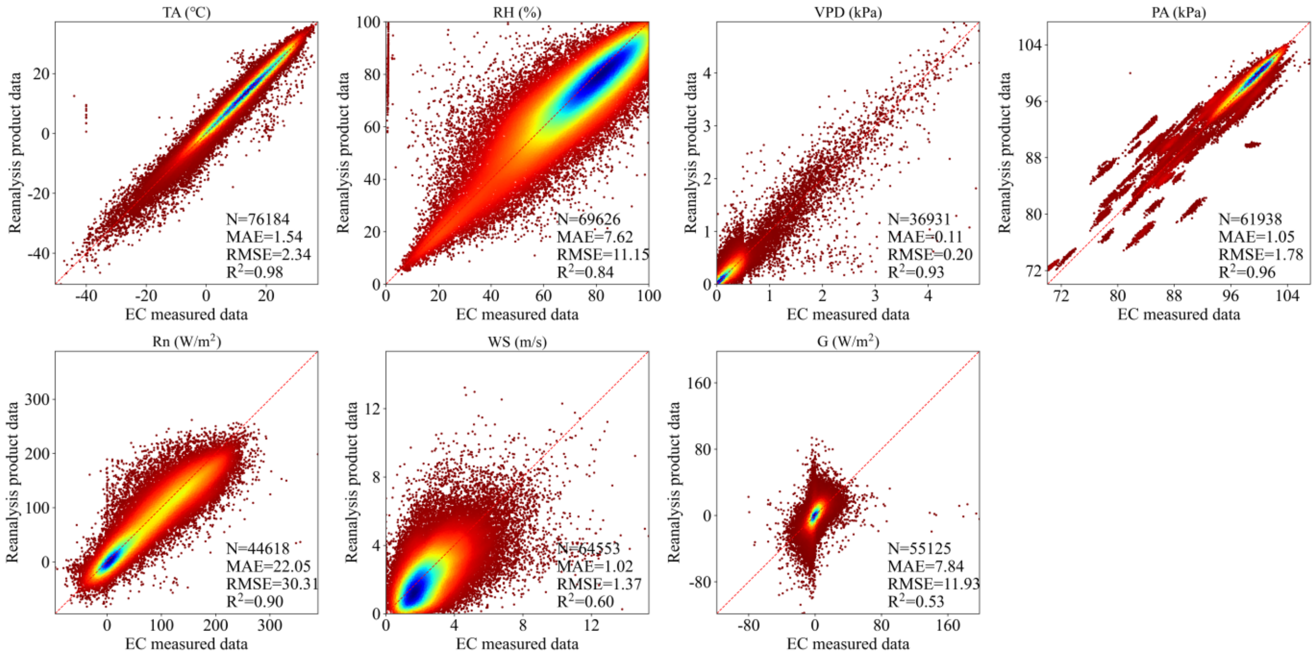


**Figure 4: Accuracy evaluation of meteorological reanalysis product.**

**Table 2: Variable information of three meteorological reanalysis products**

| Products | Variables | Descriptions |
|---|---|---|
| ERA5-Land | temperature_2m | Temperature of air at 2m |
| | dewpoint_temperature_2m | Dewpoint temperature at 2m |
| | surface_pressure | Pressure of the atmosphere. |
| | surface_net_solar_radiation_sum | Net solar radiation at the surface |
| | surface_net_thermal_radiation_sum | Net thermal radiation at the surface |
| | u_component_of_wind_10m | Eastward component of the 10m wind. |
| | v_component_of_wind_10m | Northward component of the 10m wind. |
| GLDAS-CLSM | Qg_tavg | Ground heat flux |
| MERRA-2 M2T1NXFLX | $Z_{0m}$ | Surface roughness |

### 3.2 Evaluation of the Gap-filling schedule

#### 3.2.1 Modification of the Gap-filling method

To ensure the accuracy of the filled ET partially supplemented with meteorological reanalysis products, we randomly retained 10% of the actual ET measurements at each site, and then artificially created a 50% gap within this subset to

https://doi.org/10.5194/essd-2024-291
Preprint. Discussion started: 9 August 2024


validate the full-factorial method, as depicted in Figure 5. The analysis identified outliers in the filled ET, primarily caused by instances where the observed net radiation minus ground heat flux corresponding to some of the measured ET are close to zero. These instances result in abnormal ratios of $\frac{(R_n-G)_{gap}}{(R_n-G)_{obs}}$, thereby affecting the filled ET. Additionally, Figure 5 illustrates the validation results of the filled ET data within the 5% to 95% range, demonstrating that the full-factorial method achieves high accuracy in the absence of outliers, with MAE, RMSE, and $R^2$ values of 10.95 W/m², 17.36 W/m², and 0.86, respectively. To mitigate the impact of anomalous data, the gap-filling method was modified to leverage the median. For each ET gap, all measured ET values and corresponding meteorological variables within the site are considered in the calculation, and the median of all results is used to fill this gap, as outlined in Equation 10.

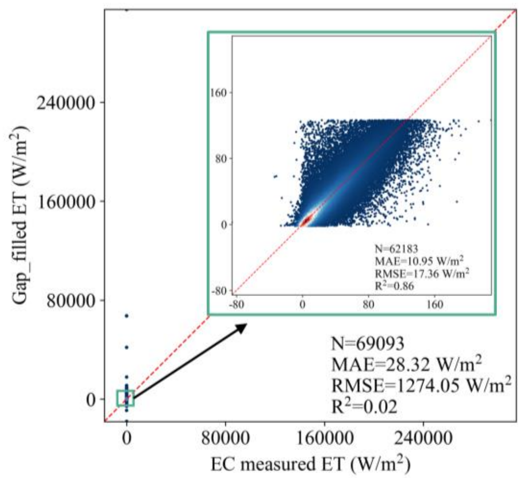


**Figure 5: Validation of filled ET using the full-factorial method based on meteorological data gap-filled from reanalysis products.**

$$ET_{\text{gap}} = \text{Median}\left\{ET_{obs_i} \times \frac{(Rn-G)_{\text{gap}}\,\Delta_{\text{gap}}}{(Rn-G)_{obs_i}\,\Delta_{obs_i}} \times \frac{(\Delta+\gamma)_{\text{gap}}}{(\Delta+\gamma)_{obs_i}} \times \frac{\beta^*_{obs_i}}{\beta^*_{gap}}\right\} \quad (10)$$

where $ET_{\text{gap}}$ is the median of all calculated $ET_{gap}$, $ET_{obs_i}$ is the i-th measurement of ET, and $Median\{\ldots\}$ means taking the median.

ET observations from sites featuring diverse land cover types were filtered before a 50% data gap was randomly introduced. The comparison of the gap-filled results with corresponding observations is shown in Figure 6. Across diverse land cover types, the modified method exhibited high precision, with MAE of 6.02~10.87 W/m², RMSE of 13.79~24.60 W/m², and $R^2$ of 0.84~0.96 for the gap-filled ET compared to the observed ET.

https://doi.org/10.5194/essd-2024-291
Preprint. Discussion started: 9 August 2024



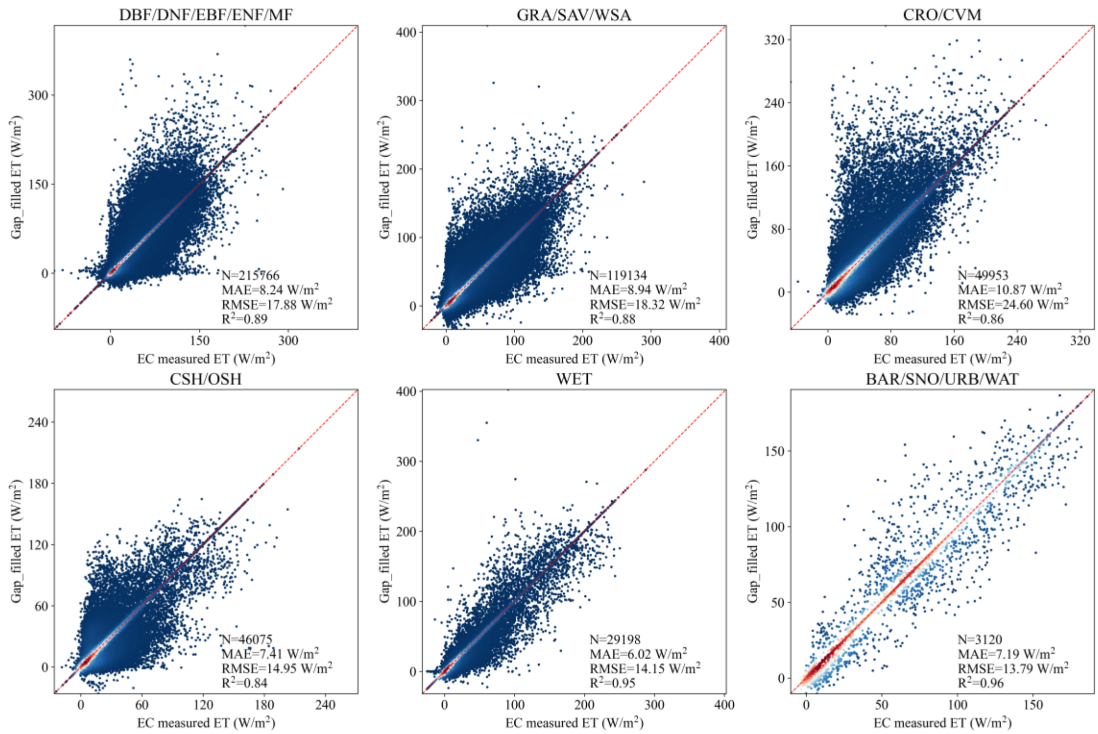


**Figure 6: Validation of the filled ET using the modified full-factorial method at diverse land cover types.**

### 3.2.2 Evaluation of gap-filled evapotranspiration

We selected several metrics for evaluating the gap-filled ET, including Mean Error (ME), Relative Mean Error (RME), Root Mean Squared Error (RMSE), Relative Root Mean Squared Error (RRMSE), Correlation Coefficient (R), and Taylor Score (TS). The closer the values of ME, RME, RMSE, and RRMSE are to 0, the smaller the deviation between the ET product and the filled ET; conversely, higher values of R and TS indicate the greater consistency (Eqs.11-18) (Elnashar et al., 2021). We ranked and scored the outcomes of these evaluation metrics based on a comparison between the filled ET and the ET products at each site. The scores for each metric from each site were then aggregated to compute the total score. Subsequently, the total scores for each site (Z_Score) were normalized to analyse the consistency and deviation between the filled ET and ET products. Additionally, we assessed the energy closure condition of the filled ET data using the Energy Balance Ratio (EBR).

$$\mathrm{ME} = \frac{1}{n}\sum_{i=1}^{n} Y_i - X_i \tag{11}$$

$$\mathrm{RME} = \frac{\mathrm{ME}}{X} \tag{12}$$

$$\mathrm{RMSE} = \sqrt{\frac{\sum_{i=1}^{n}(Y_i - X_i)^2}{n}} \tag{13}$$

$$\mathrm{RRMSE} = \frac{\mathrm{RMSE}}{X} \tag{14}$$

$$R = \frac{\sum_{i=1}^{n}\left[(Y_i - Y)(X_i - X)\right]}{\sqrt{\sum_{i=1}^{n}(Y_i - Y)^2}\sqrt{\sum_{i=1}^{n}(X_i - X)^2}} \tag{15}$$

$$\mathrm{TS} = \frac{4(1+R)}{\left(\mathrm{SD} + \frac{1}{\mathrm{SD}}\right)^2 (1+R_0)} \tag{16}$$

$$Z_s core = \frac{score - score_{min}}{score_{max} - score_{min}} \tag{17}$$

$$EBR = \frac{\sum(LE + H)}{\sum(R_n - G)} \tag{18}$$

where $n$ is the number of data; $i$ is the $i$th filled data; $X$ is the filled ET data; $Y$ is the data from the ET product, and SD is the standard deviation. $R_0$ is the maximum theoretical $R$ value (0.9976) (Taylor, 2001). $Score$ is the sum of the rankings of all metrics for each site; $score_{min}$ is the minimum scores; $score_{max}$ is the maximum scores. LE (W/m²) is the latent heat flux; and H (W/m²) is the sensible heat flux.

## 4 Results

### 4.1 Overall evaluation from comparison between gap-filled ET and ET products

Table 3 presents the evaluation metrics from the overall comparison between filled ET and ET products. Approximately 80% of sites have total score (Z_Score) values within the range of [0, 0.6). At these sites, the average |ME|

of the filled ET compared to three ET products is 0.32 mm/d, the average |RMSE| is 0.92 mm/d, and the average R is 0.79. This indicates a high consistency between the filled ET data and the three ET products at the majority of sites.

For the 75 sites with Z_Score values in the range of [0.6, 1], the differences between the filled ET data and the three ET products are significant, with an average |ME| of 3.07 mm/d, an average |RMSE| of 5.01 mm/d, and an average R of 0.31. To analyse the discrepancies between the filled ET and the three ET products (ERA5-Land, BESS, and GLEAM) at these sites, the sites were further categorized based on their performance: sites with filled ET values close to the nearby ET observations, or exhibiting similar trends in time series trends in ET observations, Leaf Area Index (LAI, from MODIS: MCD15A3H.061), and $R_n$, were categorized as Better Performance Sites; others were categorized as Uncertain Performance Sites.

**Table 3: Evaluation metrics from the comparison between filled ET and ET products**

| Z_Score | $\|ME\|_{ave}$ (mm/d) | $\|RME\|_{ave}$ (mm/d) | $\|RMSE\|_{ave}$ (mm/d) | $\|RRMSE\|_{ave}$ | $R_{ave}$ | $TS_{ave}$ | Number of sites |
|---|---|---|---|---|---|---|---|
| [0-0.1) | 0.11 | 7.02 | 0.78 | 47.09 | 0.92 | 1.31 | 12 |
| [0.1-0.2) | 0.17 | 13.16 | 0.80 | 59.11 | 0.89 | 1.30 | 26 |
| [0.2-0.3) | 0.26 | 31.90 | 0.79 | 84.86 | 0.86 | 1.41 | 58 |
| [0.3-0.4) | 0.31 | 37.65 | 0.91 | 92.16 | 0.76 | 1.33 | 56 |
| [0.4-0.5) | 0.41 | 70.91 | 0.96 | 144.37 | 0.67 | 1.35 | 59 |
| [0.5-0.6) | 0.64 | 86.72 | 1.25 | 158.58 | 0.61 | 1.25 | 53 |
| [0.6-0.7) | 0.96 | 170.21 | 1.62 | 305.02 | 0.58 | 1.13 | 41 |
| [0.7-0.8) | 1.90 | 185.60 | 3.15 | 275.13 | 0.61 | 0.77 | 15 |
| [0.8-0.9) | 2.03 | 250.63 | 3.29 | 404.25 | 0.27 | 0.45 | 14 |
| [0.9-1.0] | 7.40 | 259.15 | 11.97 | 326.60 | -0.23 | 0.36 | 5 |

## 4.2 Better performance of gap-filled ET

### 4.2.1 Better performance in temporal variations

Compared to three ET products, the filled ET at six of the 75 sites exhibited distinct seasonal variations, as shown in Figure 7. The filled ET values are essentially equivalent to the nearby measured ET values, and the differences in temporal variation trends between the filled ET and the ET products differ across various land surface types.

At crop sites (US-DS3, US-RGB, US-Rgo, and DK-Fou), ET observations clearly demonstrate the significant impact of the crop growth cycle. The filled ET at each site further mirrors the pattern of ET variations associated with crop growth,

https://doi.org/10.5194/essd-2024-291
Preprint. Discussion started: 9 August 2024


showing higher ET values during the growth period and lower values during the non-growth period. The filled ET also align with $R_n$ and LAI in their variation trends. Additionally, as these four sites are situated across different latitudinal zones, the variation in ET underscores the significant impact from climate. For instance, at the US-DS3 site, the maximum ET approaches 10 mm/d, whereas at the DK-Fou site, it peaks at only 3mm/d. Across all four sites, the three ET products exhibit similar error characteristics; they estimate ET well during the non-growing season of crops but tend to overlook the impact of crop growth on ET, particularly at the US-DS3, US-RGB, and US-Rgo sites, where ET is consistently underestimated during the crop growing season.

Two forest sites, AU-Lox and Collie, labelled as DBF and EBF, respectively, exhibit distinct variations in ET. At Site AU-Lox, ET data, along with $R_n$ and LAI, demonstrate consistent seasonal fluctuations: ET peaks from December to February and reaches its lowest from June to August, aligning with the tree growth cycle. The three ET products accurately estimated ET from June to August at this site but significantly underestimated it during other seasons due to an oversight of seasonal changes and tree growth dynamics. At Site Collie, which experiences two distinct rainy seasons, ET rates decrease from May to August, where all three ET products fail to capture the impact of the wet-dry season transition on ET and consistently overestimate it.

The gap-filled ET data at these six sites effectively captured the intricate relationship between ET, vegetation growth, and seasonal changes, demonstrating the sensitivity of ET to vegetation status and the impact of seasonal variations. Compared to the three ET products, the gap-filled ET at these sites exhibited higher accuracy and reliability.

https://doi.org/10.5194/essd-2024-291
Preprint. Discussion started: 9 August 2024


Open Access Earth System Science Data Discussions

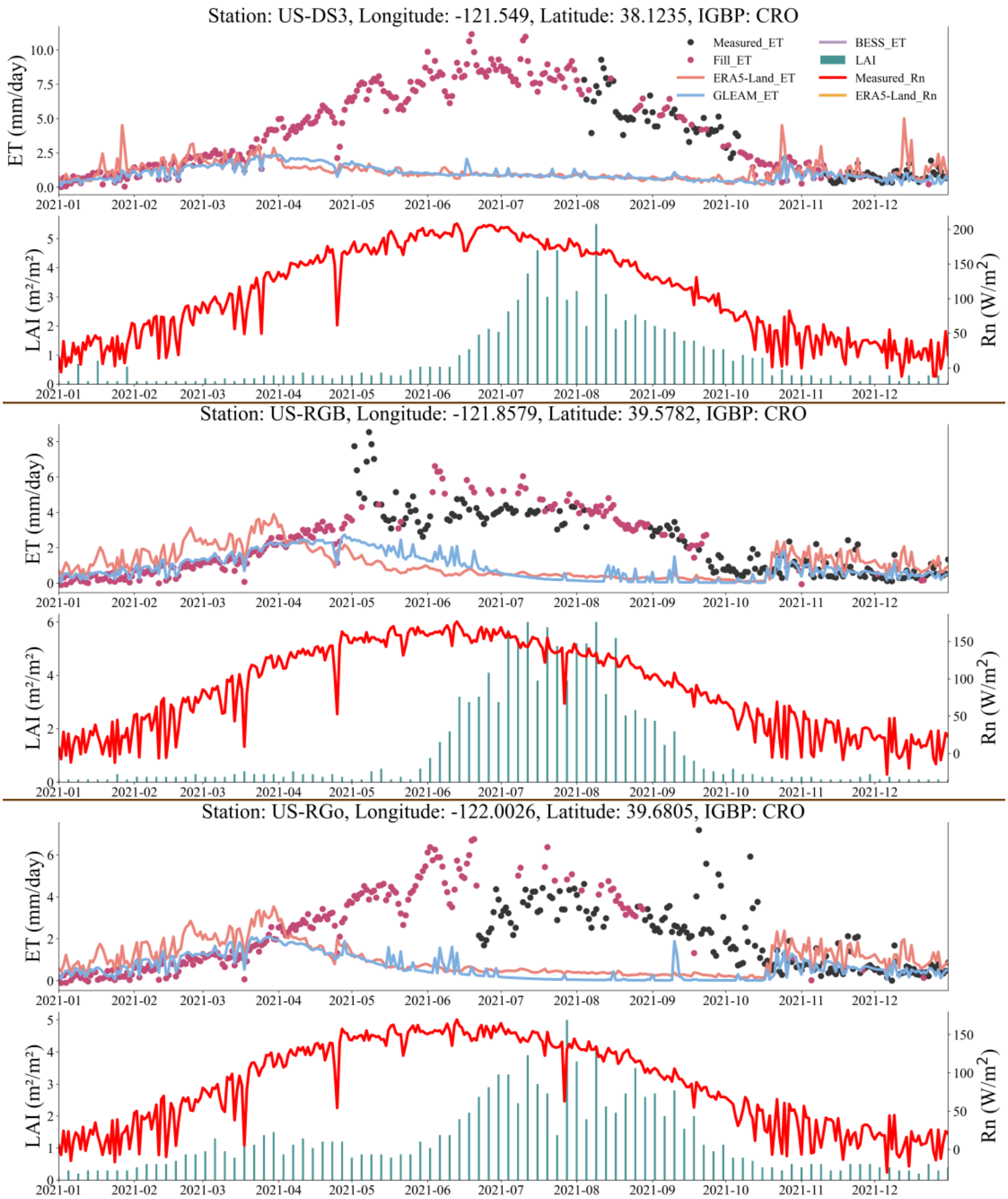


**Figure 7-1: Sites with temporal variability differences between the filled ET and ET products.**

https://doi.org/10.5194/essd-2024-291
Preprint. Discussion started: 9 August 2024

Open Access Earth System Science Data Discussions

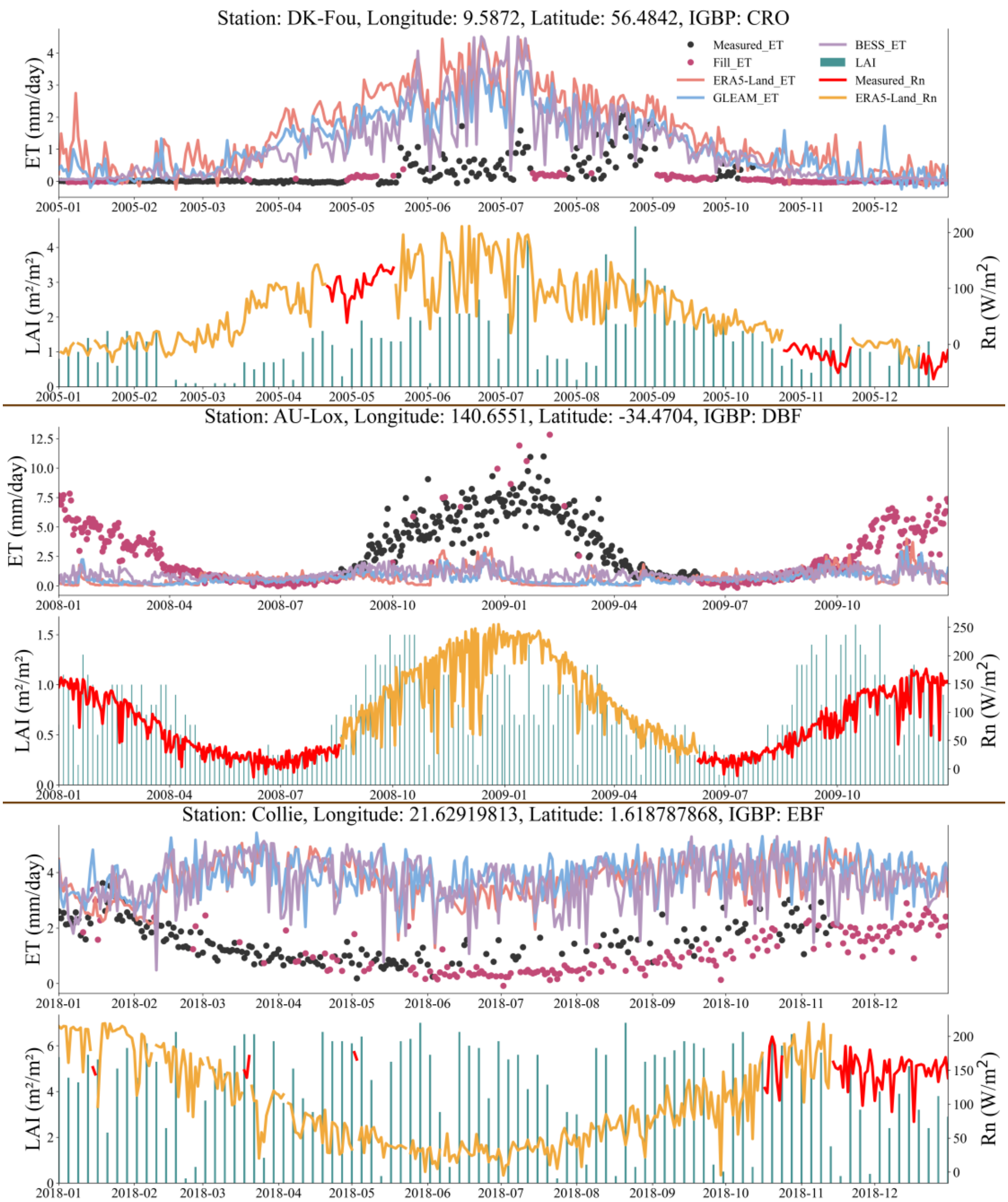


**Figure 7-2: Sites with temporal variability differences between the filled ET and ET products.**

### 4.2.2 More consistence with ET observations

Among the 43 out of 75 sites where significant differences exist between the filled ET data and the three ET products, the filled ET are generally more consistent with the ET observations in their range and seasonal trends (Figure 8 and Figure 1S). Figure 8 highlights some representative sample sites from this group.

At the US-HB3 site, the filled ET demonstrates higher consistency with adjacent ET observations compared to ET products. While GLEAM effectively simulates the seasonal trends of ET (R=0.96, Table 4), it tends to overestimate ET (MAE=2.44 mm/d, RMSE=2.70 mm/d) and also records several exceptionally high values. Conversely, although BESS demonstrates slightly lower accuracy in simulating seasonal trends compared to GLEAM (R=0.88), it exhibits higher precision, with an MAE of 0.42 mm/d and an RMSE of 0.59 mm/d.

At the US-Tw4 site, the filled ET, when compared with the ET observations from the corresponding years, shows almost identical extreme values, particularly in maintaining the ET trend through the gap-filling process in 2021. The three ET products exhibited an underestimation of ET, especially from April to October. Among these, the ERA5-Land product demonstrates relatively higher accuracy (MAE=-0.72 mm/d, RMSE=1.98 mm/d), while the BESS product more accurately simulates the ET variation trends with an R of 0.76.

At the CA-Ca1 site, the filled ET continued to accurately simulate the seasonal trends of ET, further demonstrating that the full-factorial method maintains high gap-filling accuracy, even with extended gaps. Among the three ET products, the ERA5-Land and BESS products show seasonal variation similar to those observed in the gap-filled ET and actual ET observations. In contrasts, the GLEAM product not only has large estimation errors (MAE=1.54 mm/d, RMSE=2.18 mm/d) but also failed to capture the seasonal variation trend of ET with an R of 0.35.

At the CA-DBB site, the filled ET displays a consistent range with the ET observations whereas the three ET products exhibit significant overestimations. Among these, ERA5-Land exhibits the lowest accuracy, with a MAE of 1.29 mm/d, an RMSE of 1.67 mm/d, and an R of 0.48.

Overall, the filled ET across these sites demonstrate range and seasonal trends comparable to those observed in ET observations, whereas as the three ET products exhibits variability across diverse geographic locations and vegetation types. Consequently, we consider the filled ET at these 43 sites to be highly reliable.

https://doi.org/10.5194/essd-2024-291
Preprint. Discussion started: 9 August 2024

Earth System Science Data
Open Access
Discussions

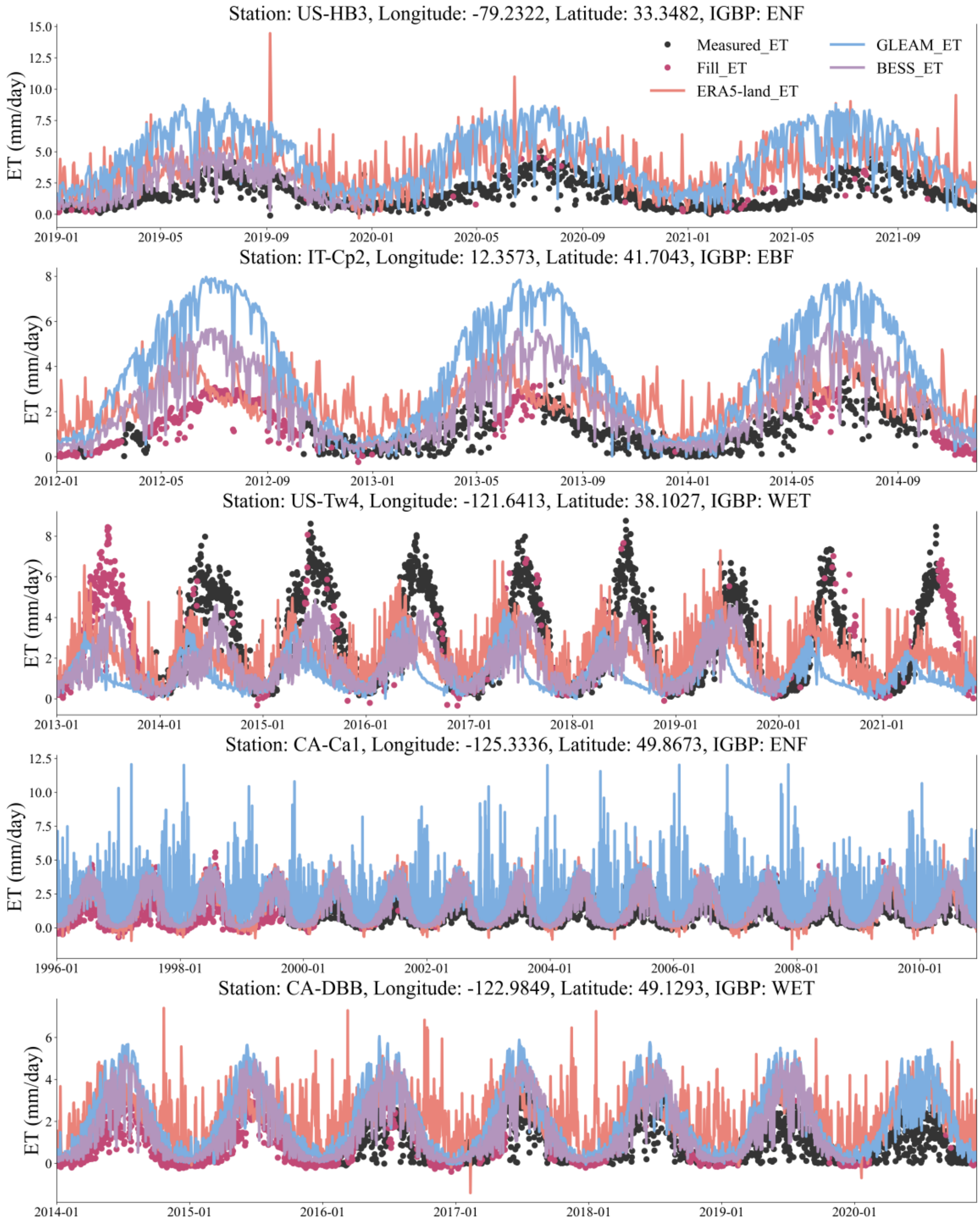


**Figure 8: Sites with value range differences between the filled ET and ET products.**

https://doi.org/10.5194/essd-2024-291
Preprint. Discussion started: 9 August 2024

Open Access Earth System Science Data Discussions

**Table 4: Statistical items from comparisons between ET products and ET observations.**

| | Station | US-HB3 | IT-Cp2 | US-Tw4 | CA-Ca1 | CA-DBB |
|---|---|---|---|---|---|---|
| MAE (mm/d) | ERA5-Land_ET | 1.78 | 1.22 | -0.72 | 0.59 | 1.29 |
| | GLEAM_ET | 2.44 | 2.90 | -1.50 | 1.54 | 0.95 |
| | BESS_ET | 0.42 | 1.41 | -0.98 | 0.49 | 0.65 |
| RMSE (mm/d) | ERA5-Land_ET | 2.27 | 1.56 | 1.98 | 0.93 | 1.67 |
| | GLEAM_ET | 2.70 | 3.36 | 2.47 | 2.18 | 1.16 |
| | BESS_ET | 0.59 | 1.68 | 1.75 | 0.74 | 0.86 |
| R | ERA5-Land_ET | 0.67 | 0.57 | 0.46 | 0.83 | 0.48 |
| | GLEAM_ET | 0.96 | 0.98 | 0.32 | 0.35 | 0.95 |
| | BESS_ET | 0.88 | 0.95 | 0.76 | 0.91 | 0.95 |

### 4.3 Uncertain performance of gap-filled ET

Uncertainty exists in the gap-filled ET at 22 of the 75 sites, primarily due to the absence of ET observations for comparison (Figure 9, Figure 2S). Figure 9 presents sample sites and analyses the reasons for their uncertainty. For instance, at the US-xSJ and ES-LMa, both classified as savannah (SAV), the temporal variation trends of the filled ET are consistent with those of $R_n$. However, when examining the temporal variation trends of measured ET and LAI, the three ET products align more closely to them, particularly noting a sharp decline in May each year. This decline is likely due to frequent fire events at these sites, as noted by Yang et al. (2023), which cause significant changes in LAI. The sharp decrease in LAI leads to reduced ET, a change not captured by the input variables of the full-factorial method, thus introducing uncertainty in the filled ET.

At the GL-ZaF and SJ-Adv sites, the temporal trends of the filled ET and ERA5-Land closely align, yet they diverge significantly from the other two ET products. Given these sites' high-latitude locations and the limited, and clustered measurements available, the accuracy of the filled ET remains uncertain.

At the ES-Ln2 site, notable differences are observed between the filled ET and the three ET products in terms of their temporal trends, which exhibit more volatility and align more closely with changes in $R_n$. The site's maximum LAI of only 0.6 and its minimal temporal trend suggest sparse surface vegetation and, theoretically, low ET (Khosa et al., 2019). Nonetheless, the reliability of the filled ET requires further verification due to scarcity of ET observations.

At the DK-Ris site, while the filled ET and the three ET products share similar temporal trends, their ranges vary significantly. The limited availability of ET observation constrains further analysis of the filled ET's reliability. The factors contributing to the uncertainty in the filled ET at this site mirror those in Figure 2S.

https://doi.org/10.5194/essd-2024-291
Preprint. Discussion started: 9 August 2024


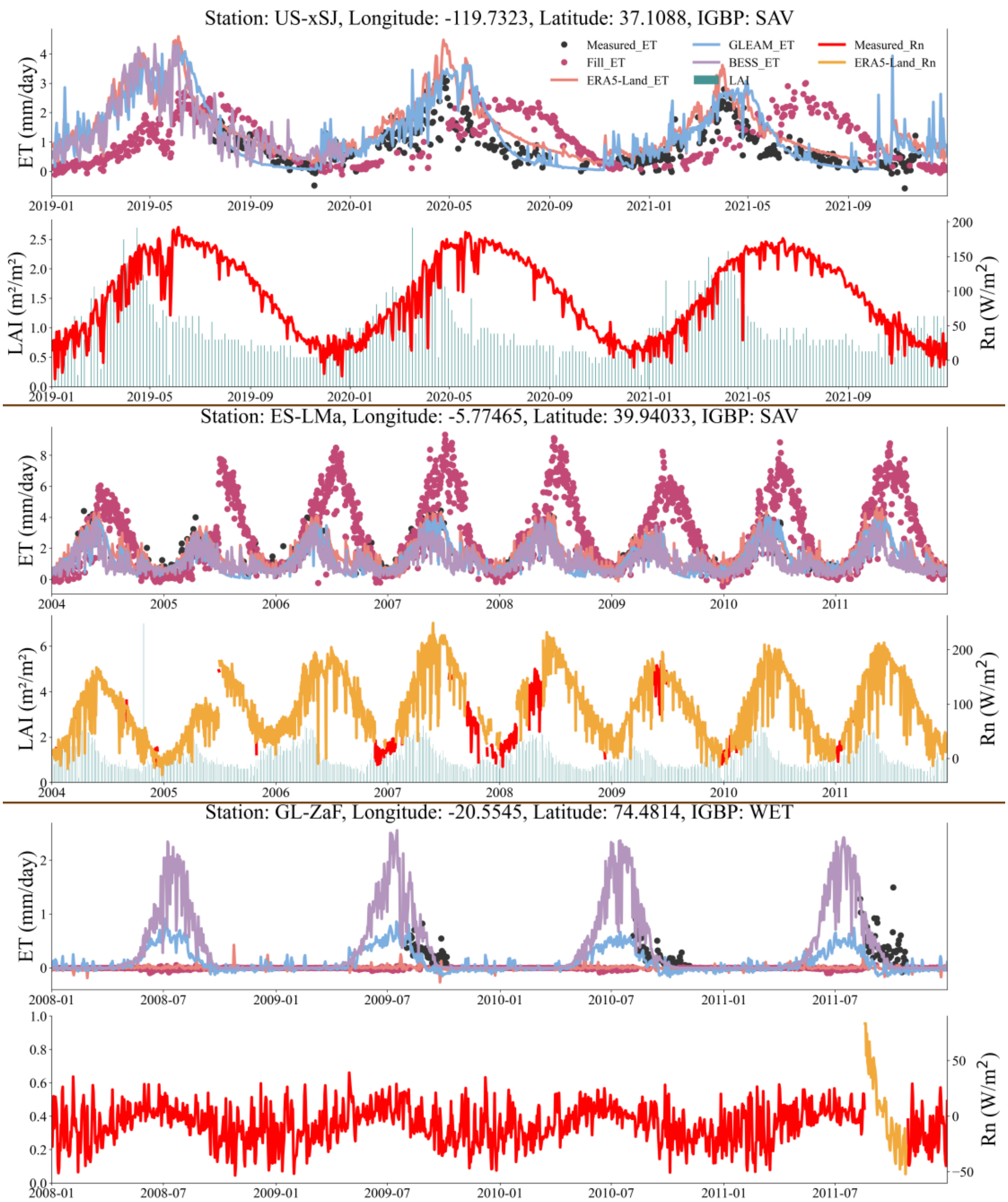


**Figure 9-1: Filled ET for uncertain sites.**

https://doi.org/10.5194/essd-2024-291
Preprint. Discussion started: 9 August 2024


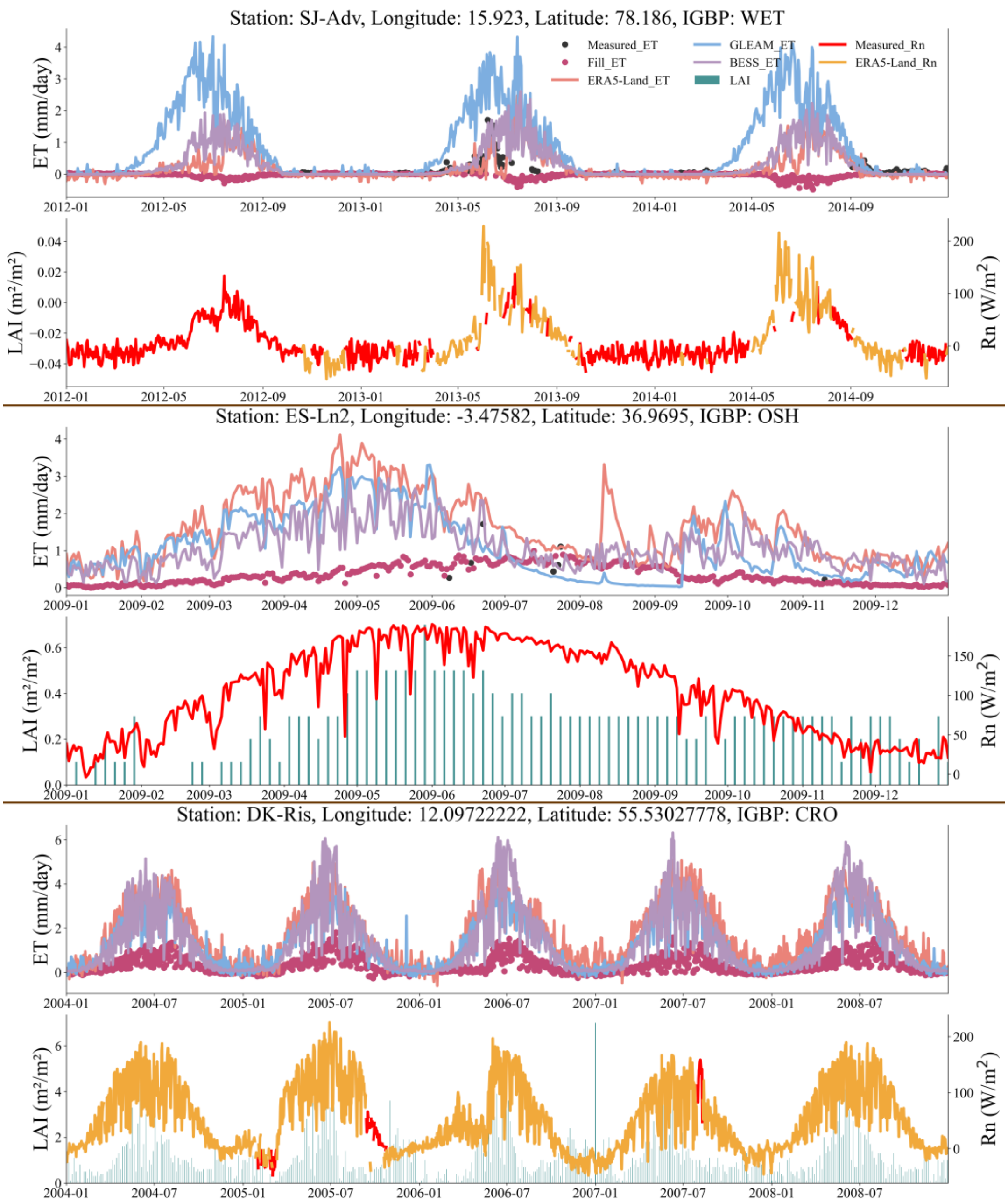


344
345 **Figure 9-2: Filled ET for uncertain sites.**

https://doi.org/10.5194/essd-2024-291
Preprint. Discussion started: 9 August 2024

Open Access Earth System Science Data Discussions

Among these uncertain sites, the CH-BaA and DE-RuW sites feature only a few days with ET observations, accompanied by corresponding negative net radiation minus ground heat flux $(R_n - G)_{obs}$ values. However, most ET gaps are associated with positive $(R_n - G)_{gap}$, resulting in predominantly negative values for the filled ET. To mitigate potential errors in filling ET, we used the absolute values of $(R_n - G)_{obs}$ from measured days to fill the gaps , as depicted in Figure 10. At these two sites, the filled ET consistently matches the seasonal variation trends of the three ET products, $R_n$, and LAI, but exhibits a broader numerical range. Given the sparse ET observations, further evaluation is necessary to assess the reliability of the filled ET at these two sites.

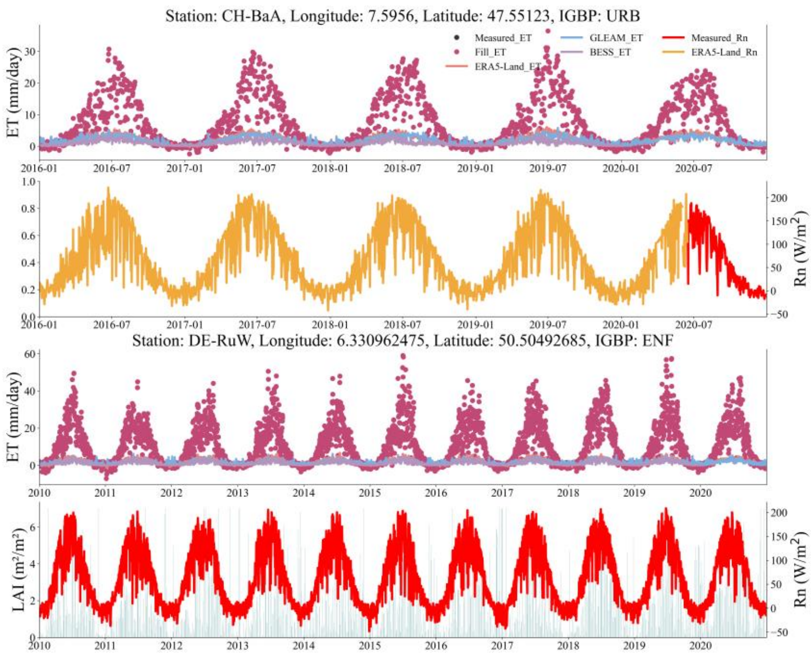


**Figure 10: Sites with special processing to avoid erroneous results.**

By comparing the temporal trends and value ranges of the filled ET and the three ET products against the measured ET, it is evident that, aside from the 26 sites where the reliability of the filled ET requires further verification, the filled ET at the remaining 313 sites is of high quality (Wang & Jiang, 2024).

### 4.4 Energy closure of well-performed gap-filled ET

To further assess the reliability of gap-filled ET, we evaluated the energy closure status at 313 sites, integrating $R_n$, H, and G data across various surface types and latitudinal zones. Figure 11 illustrates the energy balance closure of the gap-filled ET across different surface types. The determination coefficients ($R^2$) indicate a strong correlation between

https://doi.org/10.5194/essd-2024-291
Preprint. Discussion started: 9 August 2024


turbulent fluxes (LE + H) and available energy (Rn – G), with values ranging from 0.84 to 0.94. However, energy transformation efficiency varies by sites, depending on the underlying surface types. Site with wetland (WET) surface exhibit the highest energy transformation efficiency (MAE=21.66 W/m², RMSE=28.37 W/m²), while site with forest (DBF/DNF/EBF/ENF/MF) show the lowest (MAE=28.67 W/m², RMSE=36.91 W/m²). Due to the scarcity of sites categorized as barren (BAR), snow (SNO), urban (URB), and water (WAT), the Energy Balance Ratio (EBR) was not calculated for these types. overall, the energy balance closure ratios for different land cover types are satisfactory, with an average EBR of 0.79. In grassy sites (GRA/SAV/WSA), the energy balance closure is optimal, with averaged EBR of 0.84; conversely, in wetland (WET) sites, it is least effective, with averaged EBR of 0.64.

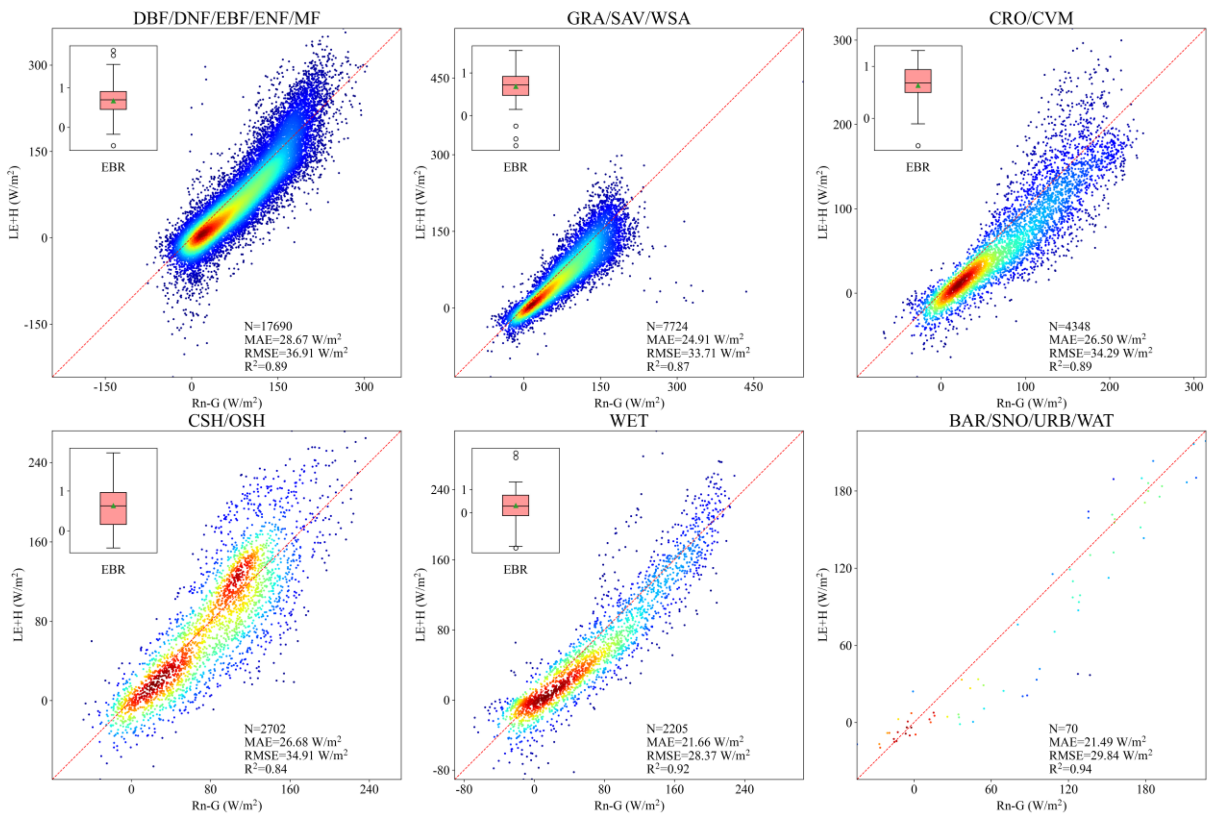


**Figure 11: Energy balance closure of gap-filled ET across different surface types.**

Figure 12 illustrates the energy balance closure of gap-filled ET across different latitude zones. Overall, the EBR tends to decrease as latitude increases. The correlation between latent and sensible heat fluxes (LE + H) and available energy (Rn – G) is notably lower in the latitude zones (10,20] and (20,30], with $R^2$ of 0.74 and 0.78, respectively. Sites within the latitude zone (70,80] display relatively high energy transformation efficiency (MAE=19.15 W/m², RMSE=26.12

https://doi.org/10.5194/essd-2024-291
Preprint. Discussion started: 9 August 2024


W/m²). In contrast, sites in other zones show comparable efficiencies, with MAE ranging from 24.34 W/m² to 29.11 W/m² and RMSE ranging from 31.31 W/m² to 37.38 W/m².

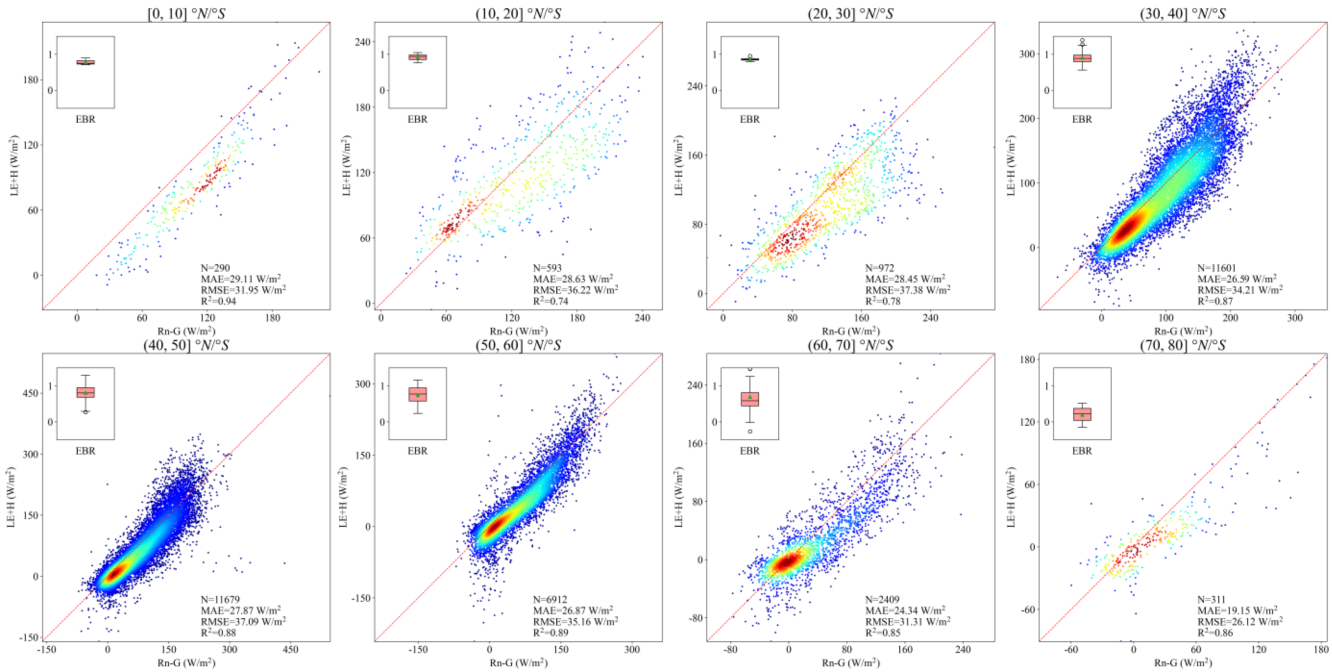


**Figure 12: Energy balance closure of gap-filled ET across different latitudinal zones.**

## 4.5 Temporal distribution of continuous ET after gap-filling

The gap-filled ET at each site has been aggregated to annual value to analyse their spatiotemporal coverage. The dataset encompasses 313 sites, categorized as follows: 131 forest sites, 80 grass sites, 42 crop sites, 32 shrub sites, 25 wetland sites, and 3 sites of other cover types (Figure 13). The duration of data at these sites ranges from 1 to 27 years. For instance, among forest sites, 41 sites have ET data spanning 1 to 4 years, 35 sites range from 5 to 8 years; 21 sites from 9 to 12 years; 19 sites from 13 to 17 years; and 15 sites have records from18 to 27 years. Similar diversity in the data record durations is observed across other land cover types.

The spatial distribution of sites across various land cover types reveals notable differences in annual average ET. Among them, annual average ET at forest sites ranges from 145 to 1259 mm, at grass sites from 143 to 1208 mm, at crop sites from 71 to 1466 mm, at shrub sites from 88 to 852 mm, and at wetland sites from 53 to 1508 mm. The magnitude of annual average ET is strongly influenced by climatic zones.

https://doi.org/10.5194/essd-2024-291
Preprint. Discussion started: 9 August 2024


Figure 13f highlights the variations in annual ET at specific sites. Specifically, in Australia, a site with water (WAT) has an annual average ET of 1241mm, with data recorded over 22 years. In the USA, a snow (SNO) site reports an annual average ET of 113mm, with data spanning 8 years. In China, a bare soil (BAR) site features an annual average ET of 231mm, with records covering 5 years.

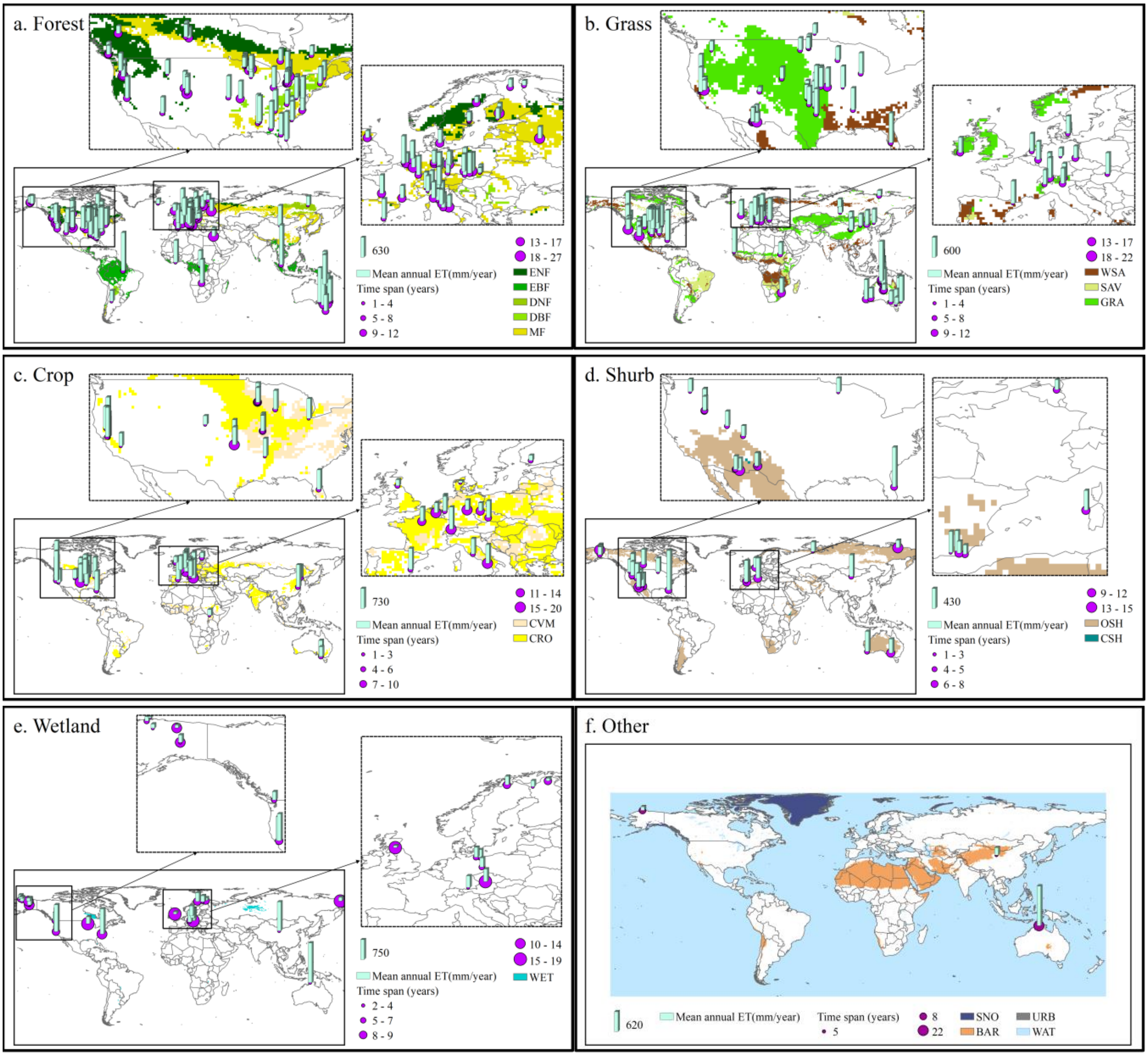


**Figure 13: Spatial distribution of continuous ET over different land cover types.**

https://doi.org/10.5194/essd-2024-291
Preprint. Discussion started: 9 August 2024


## 5 Discussion

Gaps in ET data obstruct the training and validation of ET models, as well as the accurate analysis of drivers behind ET changes (Jiang et al., 2024; Niu et al., 2024). Our statistics (Figure 3) indicate that the average gap rate of ET data from the multi-source flux network exceeds 50%, underscoring the urgency of performing gap filling to compile a continuous ET dataset. Utilizing site-measured ET and meteorological variables, along with meteorological reanalysis products, we employed a full-factorial method to fill these gaps, creating a comprehensive gap-filled ET dataset. In our evaluation, we compare the gap-filled ET with three well-known ET products and find a high degree of consistency at 80% of the sites. Significant discrepancies were also noted at some sites. Specifically, Section 4.2.1 details how the gap-filled ET data accurately continued the seasonal variations observed in the measured ET, which the three ET products failed to capture. In Section 4.2.2, the range of the gap-filled ET data closely matched the observed data, while the three ET products showed various degrees of overestimation or underestimation. These findings suggest that the full-factorial method effectively simulate the actual ET process, yielding data that closely align with actual observations.

The full-factorial method utilizes a physics-based model that comprehensively considers factors influencing ET, including meteorological conditions, vegetation characteristics, and soil state. This method simulates the actual physical process of ET through an integrated framework. By using the site-measured ET and corresponding meteorological variable data, along with meteorological data at the time of the ET gap, the filled ET were more accurately estimated. This integration is key to the method's effectiveness in filling ET gaps.

For some uncertainty noted at some sites, they are stemming from meteorological reanalysis products used to fill gaps in meteorological data. Although these products generally show good accuracy, as indicated in Figure 4, anomalies persist at individual sites, leading to reduced reliability of the filled ET at these sites in sections 4.3. Future research should aim to evaluate the performance accuracy of the meteorological reanalysis products across various sites. Additionally, comparative analyses of different products may also be necessary to further refine and validate the gap-filling process.

Another source of uncertainty arises from the failure to capture sudden changes in Leaf Area Index (LAI). Although the full-factorial method incorporates nearly all meteorological variables and uses aerodynamic resistance to reflect vegetation characteristics, it may not effectively detect rapid LAI declines caused by extreme events such as fires, especially in areas with sparse vegetation. This insensitivity can lead to significant uncertainties in ET estimates (Hu et al., 2023; Trebs et al., 2021). For instance, the sudden changes in LAI at the US-xSJ site, as depicted in Figure 9, are likely triggered by fire events. To enhance the accuracy of ET data filling, incorporating LAI data as an additional input variable will be considered to better account for the impact of such extreme events.

https://doi.org/10.5194/essd-2024-291
Preprint. Discussion started: 9 August 2024



When assessing the energy closure for ET data filling, we noted that wetland sites exhibit a relatively lower energy closure ratio due to their high moisture content, unique vegetation, and complex hydrological characteristics, creating distinctive environmental conditions that affect ET accuracy (Eichelmann et al., 2018; Wondim & Melese, 2023). Traditional ET estimation models such as the Penman-Monteith, Penman combinations, and the Priestley-Taylor often yield unsatisfactory results for wetland (Abtew, 1996; Jacobs et al., 2002). Furthermore, variances in drainage have been shown to significantly affect ET in wetlands (Wu et al., 2016). Eichelmann et al. (2018) also highlight how land cover types and structures influence ET in California wetlands. To address these challenges, the full-factorial method will be refined to include specific environmental variables for wetlands, such as water body coverage and adjusted vegetation parameters.

The energy closure ratio also exhibits a discernible correlation with latitude, showing a decreasing trend as latitude increases. This trend may attributed to the heightened complexity of climatic conditions and vegetation responses in higher latitude regions (Ma et al., 2024; Tang et al., 2024). For instance, despite numerical values of turbulent fluxes closely resembling available energy at sites within the (70, 80] latitude zone, the average Energy Balance Ratio (EBR) is only 0.2. This underscores the challenge posed by energy non-closure in high-latitude areas, which is influenced by seasonal variations, micro-meteorological diversity, radiation transmission uncertainties, and ecosystem adaptability and feedback mechanisms (Simpson et al., 2019). Therefore, future data-filling strategies should consider latitude influence, particular in polar or high-latitude areas, by employing different parameters or methods to enhance filling accuracy.

## 6 Conclusion

In this study, we utilized the full-factorial method to fill ET gaps from 339 sites from multiple flux networks, and subsequently compared the filled ET at each site with three ET products. Among these sites, 264 demonstrated high consistency between the filled ET and the ET products, with average absolute mean error (|ME|) of 0.32 mm/d, root mean square error (|RMSE|) of 0.92 mm/d, and a correlation coefficient (R) of 0.79. For the remaining 75 sites, we conducted further analysis using adjacent ET observations and the temporal trends of net radiation (Rn) and Leaf Area Index (LAI): 49 sites showed closer alignment or consistent temporal trends with nearby ET observations, while the remaining 26 sites require further verification due to issues such as insufficient input data or limited ET observations.

As a result, 313 sites exhibited relatively high-quality filled ET data, categorized as follows: 131 forest sites, 80 grass sites, 42 crop sites, 32 shrub sites, 25 wetland sites, and 3 sites of other cover types. Additionally, an energy balance closure analysis was performed, revealing an average Energy Balance Ratio (EBR) of 0.73 across these sites, indicating satisfactory energy closure.

In summary, these 313 sites with high-quality ET data filling offer robust support for ET model developments, ET product comparisons, climate change research, and other related tasks that require reliable site-specific ET data.

## Data availability

Daily evapotranspiration data for 339 global FLUXNET sites, filled with the full-factorial method, are saved in Excel files named according to the site names. In each Excel file, the column "TIMESTAMP" indicates time, while the columns "Longitude" and "Latitude" capture the geographical coordinates. The column "IGBP" details the vegetation type at the site, according to the International Geosphere-Biosphere Programme classification (Abelson, 1986), and the column "LE" indicates evapotranspiration amount ($W/m^2$). The column "LE_QC" indicates data quality (0 = measured; 1 = filled). Data from 313 sites with high-quality filled data is stored in the "Filled Data with High Quality" folder, while data from the remaining 26 sites is stored in the "Filled Data with Uncertainty" folder. The data are available for download at https://doi.org/10.57760/sciencedb.11651 (Wang & Jiang, 2024).

## Author contributions

All authors discussed the results and contributed to the paper.

## Acknowledgements

We express our gratitude to the staff at AmeriFlux, FLUXNET, EuroFlux, OzFlux, ChinaFlux, TPDC, and NCDDC for providing datasets from numerous land-cover type sites. Additionally, we thank the teams responsible for the meteorological reanalysis data from ERA5-Land (the Land component of the Fifth Generation of European Reanalysis), GLDAS (Global Land Data Assimilation System), and MERRA-2 (Modern-Era Retrospective analysis for Research and Applications, Version 2). We also appreciate the provision of three evapotranspiration products from BESSv2.0 (Breathing Earth System Simulator Version 2.0), GLEAM (Global Land Evaporation Amsterdam Model), and ERA5-Land.

## Competing interests

The authors declare that they have no conflict.

**Financial support**

This work was supported by the National Natural Science Foundation of China [42371368] and the Postgraduate Research & Practice Innovation Program of Jiangsu Province [KYCX24_1449].

## References

Abelson, P. H.: The international geosphere-biosphere program., Science, 234, 657, https://doi.org/10.1126/science.234.4777.657, 1986.

Abtew, W.: Evapotranspiration Measurements and Modeling for Three Wetland Systems in South Florida1, JAWRA Journal of the American Water Resources Association, 32, 465–473, https://doi.org/10.1111/j.1752-1688.1996.tb04044.x, 1996.

Alavi, N., Warland, J. S., and Berg, A. A.: Filling gaps in evapotranspiration measurements for water budget studies: Evaluation of a Kalman filtering approach, Agricultural and Forest Meteorology, 141, 57–66, https://doi.org/10.1016/j.agrformet.2006.09.011, 2006.

Allen, R. G., Pereira, L. S., Howell, T. A., and Jensen, M. E.: Evapotranspiration information reporting: I. Factors governing measurement accuracy, Agricultural Water Management, 98, 899–920, https://doi.org/10.1016/j.agwat.2010.12.015, 2011.

Amani, S. and Shafizadeh-Moghadam, H.: A review of machine learning models and influential factors for estimating evapotranspiration using remote sensing and ground-based data, Agricultural Water Management, 284, 108324, https://doi.org/10.1016/j.agwat.2023.108324, 2023.

Aouissi, J., Benabdallah, S., Lili Chabaâne, Z., and Cudennec, C.: Evaluation of potential evapotranspiration assessment methods for hydrological modelling with SWAT—Application in data-scarce rural Tunisia, Agricultural Water Management, 174, 39–51, https://doi.org/10.1016/j.agwat.2016.03.004, 2016.

Başakın, E. E., Ekmekcioğlu, Ö., and Özger, M.: Providing a comprehensive understanding of missing data imputation processes in evapotranspiration-related research: a systematic literature review, Hydrological Sciences Journal, 68, 2089–2104, https://doi.org/10.1080/02626667.2023.2249456, 2023.

Beringer, J., Hutley, L. B., McHugh, I., Arndt, S. K., Campbell, D., Cleugh, H. A., Cleverly, J., Resco de Dios, V., Eamus, D., Evans, B., Ewenz, C., Grace, P., Griebel, A., Haverd, V., Hinko-Najera, N., Huete, A., Isaac, P., Kanniah, K., Leuning, R., Liddell, M. J., Macfarlane, C., Meyer, W., Moore, C., Pendall, E., Phillips, A., Phillips, R. L., Prober, S. M., Restrepo-Coupe, N., Rutledge, S., Schroder, I., Silberstein, R., Southall, P., Yee, M. S., Tapper, N. J., van Gorsel, E., Vote, C.,

https://doi.org/10.5194/essd-2024-291
Preprint. Discussion started: 9 August 2024


Walker, J., and Wardlaw, T.: An introduction to the Australian and New Zealand flux tower network – OzFlux, Biogeosciences, 13, 5895–5916, https://doi.org/10.5194/bg-13-5895-2016, 2016.

Bhattarai, N., Mallick, K., Stuart, J., Vishwakarma, B. D., Niraula, R., Sen, S., and Jain, M.: An automated multi-model evapotranspiration mapping framework using remotely sensed and reanalysis data, Remote Sensing of Environment, 229, 69–92, https://doi.org/10.1016/j.rse.2019.04.026, 2019.

Chen, Y.-Y., Chu, C.-R., and Li, M.-H.: A gap-filling model for eddy covariance latent heat flux: Estimating evapotranspiration of a subtropical seasonal evergreen broad-leaved forest as an example, Journal of Hydrology, 468–469, 101–110, https://doi.org/10.1016/j.jhydrol.2012.08.026, 2012.

Drexler, J. Z., Snyder, R. L., Spano, D., and Paw U, K. T.: A review of models and micrometeorological methods used to estimate wetland evapotranspiration, Hydrological Processes, 18, 2071–2101, https://doi.org/10.1002/hyp.1462, 2004.

Eichelmann, E., Hemes, K. S., Knox, S. H., Oikawa, P. Y., Chamberlain, S. D., Sturtevant, C., Verfaillie, J., and Baldocchi, D. D.: The effect of land cover type and structure on evapotranspiration from agricultural and wetland sites in the Sacramento–San Joaquin River Delta, California, Agricultural and Forest Meteorology, 256–257, 179–195, https://doi.org/10.1016/j.agrformet.2018.03.007, 2018.

El-Madany, T. S., Reichstein, M., Perez-Priego, O., Carrara, A., Moreno, G., Pilar Martín, M., Pacheco-Labrador, J., Wohlfahrt, G., Nieto, H., Weber, U., Kolle, O., Luo, Y.-P., Carvalhais, N., and Migliavacca, M.: Drivers of spatio-temporal variability of carbon dioxide and energy fluxes in a Mediterranean savanna ecosystem, Agricultural and Forest Meteorology, 262, 258–278, https://doi.org/10.1016/j.agrformet.2018.07.010, 2018.

Elnashar, A., Wang, L., Wu, B., Zhu, W., and Zeng, H.: Synthesis of global actual evapotranspiration from 1982 to 2019, Earth Syst. Sci. Data, 13, 447–480, https://doi.org/10.5194/essd-13-447-2021, 2021.

Falge, E., Baldocchi, D., Olson, R., Anthoni, P., Aubinet, M., Bernhofer, C., Burba, G., Ceulemans, R., Clement, R., Dolman, H., Granier, A., Gross, P., Grünwald, T., Hollinger, D., Jensen, N.-O., Katul, G., Keronen, P., Kowalski, A., Lai, C. T., Law, B. E., Meyers, T., Moncrieff, J., Moors, E., Munger, J. W., Pilegaard, K., Rannik, Ü., Rebmann, C., Suyker, A., Tenhunen, J., Tu, K., Verma, S., Vesala, T., Wilson, K., and Wofsy, S.: Gap filling strategies for defensible annual sums of net ecosystem exchange, Agricultural and Forest Meteorology, 107, 43–69, https://doi.org/10.1016/S0168-1923(00)00225-2, 2001a.

Falge, E., Baldocchi, D., Olson, R., Anthoni, P., Aubinet, M., Bernhofer, C., Burba, G., Ceulemans, R., Clement, R., Dolman, H., Granier, A., Gross, P., Grünwald, T., Hollinger, D., Jensen, N.-O., Katul, G., Keronen, P., Kowalski, A., Ta Lai, C., Law, B. E., Meyers, T., Moncrieff, J., Moors, E., William Munger, J., Pilegaard, K., Rannik, Ü., Rebmann, C., Suyker, A., Tenhunen, J., Tu, K., Verma, S., Vesala, T., Wilson, K., and Wofsy, S.: Gap filling strategies for long term

https://doi.org/10.5194/essd-2024-291
Preprint. Discussion started: 9 August 2024


energy flux data sets, Agricultural and Forest Meteorology, 107, 71–77, https://doi.org/10.1016/S0168-1923(00)00235-5, 2001b.

Foltýnová, L., Fischer, M., and McGloin, R. P.: Recommendations for gap-filling eddy covariance latent heat flux measurements using marginal distribution sampling, Theor Appl Climatol, 139, 677–688, https://doi.org/10.1007/s00704-019-02975-w, 2020.

Govender, T., Dube, T., and Shoko, C.: Remote sensing of land use-land cover change and climate variability on hydrological processes in Sub-Saharan Africa: key scientific strides and challenges, Geocarto International, 37, 10925–10949, https://doi.org/10.1080/10106049.2022.2043451, 2022.

Granata, F.: Evapotranspiration evaluation models based on machine learning algorithms—A comparative study, Agricultural Water Management, 217, 303–315, https://doi.org/10.1016/j.agwat.2019.03.015, 2019.

Graveline, V., Helbig, M., Gosselin, G. H., Alcock, H., Detto, M., Walker, B., Marsh, P., and Sonnentag, O.: Surface-atmosphere energy exchanges and their effects on surface climate and atmospheric boundary layer characteristics in the forest-tundra ecotone in northwestern Canada, Agricultural and Forest Meteorology, 350, 109996, https://doi.org/10.1016/j.agrformet.2024.109996, 2024.

Helbig, M., Gerken, T., Beamesderfer, E. R., Baldocchi, D. D., Banerjee, T., Biraud, S. C., Brown, W. O. J., Brunsell, N. A., Burakowski, E. A., Burns, S. P., Butterworth, B. J., Chan, W. S., Davis, K. J., Desai, A. R., Fuentes, J. D., Hollinger, D. Y., Kljun, N., Mauder, M., Novick, K. A., Perkins, J. M., Rahn, D. A., Rey-Sanchez, C., Santanello, J. A., Scott, R. L., Seyednasrollah, B., Stoy, P. C., Sullivan, R. C., De Arellano, J. V.-G., Wharton, S., Yi, C., and Richardson, A. D.: Integrating continuous atmospheric boundary layer and tower-based flux measurements to advance understanding of land-atmosphere interactions, Agricultural and Forest Meteorology, 307, 108509, https://doi.org/10.1016/j.agrformet.2021.108509, 2021.

Hu, X., Shi, L., Lian, X., and Bian, J.: Parameter variability across different timescales in the energy balance-based model and its effect on evapotranspiration estimation, Science of The Total Environment, 871, 161919, https://doi.org/10.1016/j.scitotenv.2023.161919, 2023.

Jacobs, J. M., Myers, D. A., Anderson, M. C., and Diak, G. R.: GOES surface insolation to estimate wetlands evapotranspiration, Journal of Hydrology, 266, 53–65, https://doi.org/10.1016/S0022-1694(02)00117-8, 2002.

Jarvis, A. J., Stauch, V. J., Schulz, K., and Young, P. C.: The seasonal temperature dependency of photosynthesis and respiration in two deciduous forests, Global Change Biology, 10, 939–950, https://doi.org/10.1111/j.1529-8817.2003.00743.x, 2004.

https://doi.org/10.5194/essd-2024-291
Preprint. Discussion started: 9 August 2024


Jiang, X., Wang, Y., A., Y., Wang, G., Zhang, X., Ma, G., Duan, L., and Liu, K.: Optimizing actual evapotranspiration simulation to identify evapotranspiration partitioning variations: A fusion of physical processes and machine learning techniques, Agricultural Water Management, 295, 108755, https://doi.org/10.1016/j.agwat.2024.108755, 2024.

Jiang, Y., Tang, R., and Li, Z.-L.: A physical full-factorial scheme for gap-filling of eddy covariance measurements of daytime evapotranspiration, Agricultural and Forest Meteorology, 323, 109087, https://doi.org/10.1016/j.agrformet.2022.109087, 2022.

Katul, G., Lai, C.-T., Schäfer, K., Vidakovic, B., Albertson, J., Ellsworth, D., and Oren, R.: Multiscale analysis of vegetation surface fluxes: from seconds to years, Advances in Water Resources, 24, 1119–1132, https://doi.org/10.1016/S0309-1708(01)00029-X, 2001.

Khosa, F. V., Feig, G. T., van der Merwe, M. R., Mateyisi, M. J., Mudau, A. E., and Savage, M. J.: Evaluation of modeled actual evapotranspiration estimates from a land surface, empirical and satellite-based models using *in situ* observations from a South African semi-arid savanna ecosystem, Agricultural and Forest Meteorology, 279, 107706, https://doi.org/10.1016/j.agrformet.2019.107706, 2019.

Kim, S., Anabalón, A., and Sharma, A.: An Assessment of Concurrency in Evapotranspiration Trends across Multiple Global Datasets, Journal of Hydrometeorology, 22, 231–244, https://doi.org/10.1175/JHM-D-20-0059.1, 2021.

Koppa, A., Rains, D., Hulsman, P., Poyatos, R., and Miralles, D. G.: A deep learning-based hybrid model of global terrestrial evaporation, Nat Commun, 13, 1912, https://doi.org/10.1038/s41467-022-29543-7, 2022.

Kunwor, S., Starr, G., Loescher, H. W., and Staudhammer, C. L.: Preserving the variance in imputed eddy-covariance measurements: Alternative methods for defensible gap filling, Agricultural and Forest Meteorology, 232, 635–649, https://doi.org/10.1016/j.agrformet.2016.10.018, 2017.

Li, H., Zhang, F., Zhu, J., Guo, X., Li, Y., Lin, L., Zhang, L., Yang, Y., Li, Y., Cao, G., Zhou, H., and Du, M.: Precipitation rather than evapotranspiration determines the warm-season water supply in an alpine shrub and an alpine meadow, Agricultural and Forest Meteorology, 300, 108318, https://doi.org/10.1016/j.agrformet.2021.108318, 2021.

Li, S., Wang, G., Sun, S., Chen, H., Bai, P., Zhou, S., Huang, Y., Wang, J., and Deng, P.: Assessment of Multi-Source Evapotranspiration Products over China Using Eddy Covariance Observations, Remote Sensing, 10, 1692, https://doi.org/10.3390/rs10111692, 2018.

Long, D., Longuevergne, L., and Scanlon, B. R.: Uncertainty in evapotranspiration from land surface modeling, remote sensing, and GRACE satellites, Water Resources Research, 50, 1131–1151, https://doi.org/10.1002/2013WR014581, 2014.

Ma, L., Yu, G., Chen, Z., Yang, M., Hao, T., Zhu, X., Zhang, W., Lin, Q., Liu, Z., Han, L., Dou, X., Sun, M., Lin, Y., Luo, W., and Zhou, W.: Cascade effects of climate and vegetation influencing the spatial variation of evapotranspiration in China, Agricultural and Forest Meteorology, 344, 109826, https://doi.org/10.1016/j.agrformet.2023.109826, 2024.

https://doi.org/10.5194/essd-2024-291
Preprint. Discussion started: 9 August 2024


Majozi, N. P., Mannaerts, C. M., Ramoelo, A., Mathieu, R., Mudau, A. E., and Verhoef, W.: An Intercomparison of Satellite-Based Daily Evapotranspiration Estimates under Different Eco-Climatic Regions in South Africa, Remote Sensing, 9, 307, https://doi.org/10.3390/rs9040307, 2017.

Monson, R. K., Turnipseed, A. A., Sparks, J. P., Harley, P. C., Scott-Denton, L. E., Sparks, K., and Huxman, T. E.: Carbon sequestration in a high-elevation, subalpine forest, Global Change Biology, 8, 459–478, https://doi.org/10.1046/j.1365-2486.2002.00480.x, 2002.

Morton, F. I.: Operational estimates of areal evapotranspiration and their significance to the science and practice of hydrology, Journal of Hydrology, 66, 1–76, https://doi.org/10.1016/0022-1694(83)90177-4, 1983.

Mu, Q., Zhao, M., and Running, S. W.: Improvements to a MODIS global terrestrial evapotranspiration algorithm, Remote Sensing of Environment, 115, 1781–1800, https://doi.org/10.1016/j.rse.2011.02.019, 2011.

Niu, X., Chen, Z., Pang, Y., Niu, B., Yan, C., and Liu, S.: Environmental and biological controls on the interannual variations of evapotranspiration in a natural oak forest, Agricultural and Forest Meteorology, 349, 109969, https://doi.org/10.1016/j.agrformet.2024.109969, 2024.

Nkiaka, E., Bryant, R. G., Ntajal, J., and Biao, E. I.: Evaluating the accuracy of gridded water resources reanalysis and evapotranspiration products for assessing water security in poorly gauged basins, Hydrology and Earth System Sciences, 26, 5899–5916, https://doi.org/10.5194/hess-26-5899-2022, 2022.

Novick, K. A., Biederman, J. A., Desai, A. R., Litvak, M. E., Moore, D. J. P., Scott, R. L., and Torn, M. S.: The AmeriFlux network: A coalition of the willing, Agricultural and Forest Meteorology, 249, 444–456, https://doi.org/10.1016/j.agrformet.2017.10.009, 2018.

Novick, K. A., Metzger, S., Anderegg, W. R. L., Barnes, M., Cala, D. S., Guan, K., Hemes, K. S., Hollinger, D. Y., Kumar, J., Litvak, M., Lombardozzi, D., Normile, C. P., Oikawa, P., Runkle, B. R. K., Torn, M., and Wiesner, S.: Informing Nature-based Climate Solutions for the United States with the best-available science, Global Change Biology, 28, 3778–3794, https://doi.org/10.1111/gcb.16156, 2022.

Pan, X., Guo, X., Li, X., Niu, X., Yang, X., Feng, M., Che, T., Jin, R., Ran, Y., Guo, J., Hu, X., and Wu, A.: National Tibetan Plateau Data Center: Promoting Earth System Science on the Third Pole, Bulletin of the American Meteorological Society, 102, E2062–E2078, https://doi.org/10.1175/BAMS-D-21-0004.1, 2021.

Pastorello, G., Trotta, C., Canfora, E., Chu, H., Christianson, D., Cheah, Y.-W., Poindexter, C., Chen, J., Elbashandy, A., Humphrey, M., Isaac, P., Polidori, D., Reichstein, M., Ribeca, A., van Ingen, C., Vuichard, N., Zhang, L., Amiro, B., Ammann, C., Arain, M. A., Ardö, J., Arkebauer, T., Arndt, S. K., Arriga, N., Aubinet, M., Aurela, M., Baldocchi, D., Barr, A., Beamesderfer, E., Marchesini, L. B., Bergeron, O., Beringer, J., Bernhofer, C., Berveiller, D., Billesbach, D., Black, T. A., Blanken, P. D., Bohrer, G., Boike, J., Bolstad, P. V., Bonal, D., Bonnefond, J.-M., Bowling, D. R., Bracho, R., Brodeur, J., Brümmer, C., Buchmann, N., Burban, B., Burns, S. P., Buysse, P., Cale, P., Cavagna, M., Cellier, P., Chen, S., Chini, I., Christensen, T. R., Cleverly, J., Collalti, A., Consalvo, C., Cook, B. D., Cook, D., Coursolle, C., Cremonese, E., Curtis, P. S., D'Andrea, E., da Rocha, H., Dai, X., Davis, K. J., Cinti, B. D., Grandcourt, A. de, Ligne, A. D., De Oliveira, R. C., Delpierre, N., Desai, A. R., Di Bella, C. M., Tommasi, P. di, Dolman, H., Domingo, F., Dong, G., Dore, S., Duce, P., Dufrêne, E., Dunn, A., Dušek, J., Eamus, D., Eichelmann, U., ElKhidir, H. A. M., Eugster, W., Ewenz, C. M., Ewers, B., Famulari, D., Fares, S., Feigenwinter, I., Feitz, A., Fensholt, R., Filippa, G., Fischer, M., Frank, J., Galvagno, M., et al.: The FLUXNET2015 dataset and the ONEFlux processing pipeline for eddy covariance data, Sci Data, 7, 225, https://doi.org/10.1038/s41597-020-0534-3, 2020.

Peerbhai, T., Chetty, K. T., Clark, D. J., and Gokool, S.: Estimating evapotranspiration using earth observation data: A comparison between hydrological and energy balance modelling approaches, Journal of Hydrology, 613, 128347, https://doi.org/10.1016/j.jhydrol.2022.128347, 2022.

Polhamus, A., Fisher, J. B., and Tu, K. P.: What controls the error structure in evapotranspiration models?, Agricultural and Forest Meteorology, 169, 12–24, https://doi.org/10.1016/j.agrformet.2012.10.002, 2013.

Qian, L., Zhang, Z., Wu, L., Fan, S., Yu, X., Liu, X., Ba, Y., Ma, H., and Wang, Y.: High uncertainty of evapotranspiration products under extreme climatic conditions, Journal of Hydrology, 626, 130332, https://doi.org/10.1016/j.jhydrol.2023.130332, 2023.

Rummler, T., Arnault, J., Gochis, D., and Kunstmann, H.: Role of Lateral Terrestrial Water Flow on the Regional Water Cycle in a Complex Terrain Region: Investigation With a Fully Coupled Model System, Journal of Geophysical Research: Atmospheres, 124, 507–529, https://doi.org/10.1029/2018JD029004, 2019.

Simpson, G., Runkle, B. R. K., Eckhardt, T., and Kutzbach, L.: Evaluating closed chamber evapotranspiration estimates against eddy covariance measurements in an arctic wetland, Journal of Hydrology, 578, 124030, https://doi.org/10.1016/j.jhydrol.2019.124030, 2019.

Stauch, V. J. and Jarvis, A. J.: A semi-parametric gap-filling model for eddy covariance CO2 flux time series data, Global Change Biology, 12, 1707–1716, https://doi.org/10.1111/j.1365-2486.2006.01227.x, 2006.

Talib, A., Desai, A. R., Huang, J., Thom, J., Panuska, J. C., and Stoy, Paul. C.: Improving parameterization of an evapotranspiration estimation model with eddy covariance measurements for a regional irrigation scheduling program, Agricultural and Forest Meteorology, 350, 109967, https://doi.org/10.1016/j.agrformet.2024.109967, 2024.

Tang, R., Peng, Z., Liu, M., Li, Z.-L., Jiang, Y., Hu, Y., Huang, L., Wang, Y., Wang, J., Jia, L., Zheng, C., Zhang, Y., Zhang, K., Yao, Y., Chen, X., Xiong, Y., Zeng, Z., and Fisher, J. B.: Spatial-temporal patterns of land surface evapotranspiration from global products, Remote Sensing of Environment, 304, 114066, https://doi.org/10.1016/j.rse.2024.114066, 2024.

https://doi.org/10.5194/essd-2024-291
Preprint. Discussion started: 9 August 2024


Taylor, K. E.: Summarizing multiple aspects of model performance in a single diagram, Journal of Geophysical Research: Atmospheres, 106, 7183–7192, https://doi.org/10.1029/2000JD900719, 2001.

Trebs, I., Mallick, K., Bhattarai, N., Sulis, M., Cleverly, J., Woodgate, W., Silberstein, R., Hinko-Najera, N., Beringer, J., Meyer, W. S., Su, Z., and Boulet, G.: The role of aerodynamic resistance in thermal remote sensing-based evapotranspiration models, Remote Sensing of Environment, 264, 112602, https://doi.org/10.1016/j.rse.2021.112602, 2021.

Valentín, F., Sánchez, J. M., Martínez-Moreno, A., Intrigliolo, D. S., Buesa, I., and López-Urrea, R.: Using on-the-ground surface energy balance to monitor vine water status and evapotranspiration under deficit irrigation and rainfed conditions, Agricultural Water Management, 281, 108240, https://doi.org/10.1016/j.agwat.2023.108240, 2023.

Wan, Z., Zhang, K., Xue, X., Hong, Z., Hong, Y., and Gourley, J. J.: Water balance-based actual evapotranspiration reconstruction from ground and satellite observations over the conterminous United States, Water Resources Research, 51, 6485–6499, https://doi.org/10.1002/2015WR017311, 2015.

Wang, K. and Dickinson, R. E.: A review of global terrestrial evapotranspiration: Observation, modeling, climatology, and climatic variability, Reviews of Geophysics, 50, https://doi.org/10.1029/2011RG000373, 2012.

Wang, X. and Jiang, Y.: Gap-Filling for Daily Evapotranspiration Observations with full-factorial method at Global Flux Sites, https://doi.org/10.57760/sciencedb.11651, 2024.

Wilson, K. B. and Baldocchi, D. D.: Comparing independent estimates of carbon dioxide exchange over 5 years at a deciduous forest in the southeastern United States, Journal of Geophysical Research: Atmospheres, 106, 34167–34178, https://doi.org/10.1029/2001JD000624, 2001.

Winck, B. R., Bloor, J. M. G., and Klumpp, K.: Eighteen years of upland grassland carbon flux data: reference datasets, processing, and gap-filling procedure, Sci Data, 10, 311, https://doi.org/10.1038/s41597-023-02221-z, 2023.

Wondim, Y. K. and Melese, A. W.: Evaluation of the evapotranspiration rate of lacustrine wetland macrophytes in Lake Tana, Ethiopia, Ecohydrology & Hydrobiology, 23, 623–634, https://doi.org/10.1016/j.ecohyd.2023.05.003, 2023.

Wu, C.-L., Shukla, S., and Shrestha, N. K.: Evapotranspiration from drained wetlands with different hydrologic regimes: Drivers, modeling, and storage functions, Journal of Hydrology, 538, 416–428, https://doi.org/10.1016/j.jhydrol.2016.04.027, 2016.

Wu, J., Feng, Y., Zheng, C., and Zeng, Z.: Dense flux observations reveal the incapability of evapotranspiration products to capture the heterogeneity of evapotranspiration, Journal of Hydrology, 622, 129743, https://doi.org/10.1016/j.jhydrol.2023.129743, 2023.

Wutzler, T., Lucas-Moffat, A., Migliavacca, M., Knauer, J., Sickel, K., Šigut, L., Menzer, O., and Reichstein, M.: Basic and extensible post-processing of eddy covariance flux data with REddyProc, Biogeosciences, 15, 5015–5030, https://doi.org/10.5194/bg-15-5015-2018, 2018.

Xie, Z., Yao, Y., Tang, Q., Liu, M., Fisher, J. B., Chen, J., Zhang, X., Jia, K., Li, Y., Shang, K., Jiang, B., Yang, J., Yu, R., Zhang, X., Guo, X., Liu, L., Ning, J., Fan, J., and Zhang, L.: Evaluation of seven satellite-based and two reanalysis global terrestrial evapotranspiration products, Journal of Hydrology, 630, 130649, https://doi.org/10.1016/j.jhydrol.2024.130649, 2024.

Xing, Z., Bourque, C. P.-A., Meng, F.-R., Cox, R. M., Swift, D. E., Zha, T., and Chow, L.: A process-based model designed for filling of large data gaps in tower-based measurements of net ecosystem productivity, Ecological Modelling, 213, 165–179, https://doi.org/10.1016/j.ecolmodel.2007.11.018, 2008.

Xiong, Y., Feng, F., Fang, Y., Qiu, G., Zhao, S., and Yao, Y.: Critical Problems When Applying Remotely Sensed Evapotranspiration Products, Remote Sensing Technology and Application, 36, 121–131, https://doi.org/10.11873/j.issn.1004-0323.2021.1.0121, 2021.

Yang, X., Zhao, C., Zhao, W., Fan, H., and Yang, Y.: Characterization of global fire activity and its spatiotemporal patterns for different land cover types from 2001 to 2020, Environmental Research, 227, 115746, https://doi.org/10.1016/j.envres.2023.115746, 2023.

Yeonuk, K., S, J. M., H, K. S., Andrew, B. T., J, D. H., Minseok, K., Joon, K., and Dennis, B.: Gap-filling approaches for eddy covariance methane fluxes: A comparison of three machine learning algorithms and a traditional method with principal component analysis, Global change biology, 26, 2020.

Yu, G., Fu, Y., Sun, **aomin, Wen, X., and Zhang, L.: Recent progress and future directions of ChinaFLUX, SCI CHINA SER D, 49, 1–23, https://doi.org/10.1007/s11430-006-8001-3, 2006a.

Yu, G.-R., Wen, X.-F., Sun, X.-M., Tanner, B. D., Lee, X., and Chen, J.-Y.: Overview of ChinaFLUX and evaluation of its eddy covariance measurement, Agricultural and Forest Meteorology, 137, 125–137, https://doi.org/10.1016/j.agrformet.2006.02.011, 2006b.

Zhang, K., Kimball, J. S., and Running, S. W.: A review of remote sensing based actual evapotranspiration estimation, WIREs Water, 3, 834–853, https://doi.org/10.1002/wat2.1168, 2016.

Zhang, Q., Liu, X., Zhou, K., Zhou, Y., Gentine, P., Pan, M., and Katul, G. G.: Solar-induced chlorophyll fluorescence sheds light on global evapotranspiration, Remote Sensing of Environment, 305, 114061, https://doi.org/10.1016/j.rse.2024.114061, 2024.

https://doi.org/10.5194/essd-2024-291
Preprint. Discussion started: 9 August 2024


Zheng, M., Chen, X., Ruan, W., Yao, H., Gu, Z., Geng, K., Li, X., Deng, H., Chen, Y., and Liu, M.: Spatiotemporal variation of water cycle components in Minjiang River Basin based on a correction method for evapotranspiration products, Journal of Hydrology: Regional Studies, 50, 101575, https://doi.org/10.1016/j.ejrh.2023.101575, 2023.

Zhu, S., Clement, R., McCalmont, J., Davies, C. A., and Hill, T.: Stable gap-filling for longer eddy covariance data gaps: A globally validated machine-learning approach for carbon dioxide, water, and energy fluxes, Agricultural and Forest Meteorology, 314, 108777, https://doi.org/10.1016/j.agrformet.2021.108777, 2022a.

Zhu, W., Tian, S., Wei, J., Jia, S., and Song, Z.: Multi-scale evaluation of global evapotranspiration products derived from remote sensing images: Accuracy and uncertainty, Journal of Hydrology, 611, 127982, https://doi.org/10.1016/j.jhydrol.2022.127982, 2022b.